Heliyon 10 (2024) e34654

Contents lists available at ScienceDirect

Heliyon

journal homepage: www.cell.com/heliyon

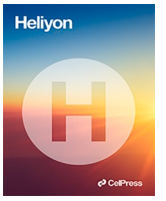

Review article

Potential applications for photoacoustic imaging using functional nanoparticles: A comprehensive overview

Pavan Mohan Neelamraju [a,1], Karthikay Gundepudi [a,1], Pradyut Kumar Sanki [a], Kumar Babu Busi [b], Tapan Kumar Mistri [c], Sambasivam Sangaraju [d], Goutam Kumar Dalapati [e], Krishna Kanta Ghosh [f], Siddhartha Ghosh [g,***], Writoban Basu Ball [h,**], Sabyasachi Chakrabortty [b,*]

[a] Department of Electronics and Communication Engineering, SRM University AP Andhra Pradesh, Andhra Pradesh, 522240, India
[b] Department of Chemistry, SRM University AP Andhra Pradesh, Andhra Pradesh, 522240, India
[c] Department of Chemistry, SRM Institute of Science and Technology, Kattankulathur, Chennai, Tamil Nadu, 603203, India
[d] National Water and Energy Center, United Arab Emirates University, Al Ain, 15551, United Arab Emirates
[e] Center for Nanofibers and Nanotechnology, Mechanical Engineering Department, National University of Singapore, Singapore, 117576
[f] Lee Kong Chian School of Medicine, Nanyang Technological University, 59 Nanyang Drive, Singapore, 636921
[g] Department of Physics, SRM University AP Andhra Pradesh, Andhra Pradesh, 522240, India
[h] Department of Biological Sciences, SRM University AP Andhra Pradesh, Andhra Pradesh, 522240, India

ARTICLE INFO

Keywords:
Photoacoustic effect
Photoacoustic signal
Photoacoustic imaging
Nanoparticles
Nanostructures alloys

ABSTRACT

This paper presents a comprehensive overview of the potential applications for Photo-Acoustic (PA) imaging employing functional nanoparticles. The exploration begins with an introduction to nanotechnology and nanomaterials, highlighting the advancements in these fields and their crucial role in shaping the future. A detailed discussion of the various types of nanomaterials and their functional properties sets the stage for a thorough examination of the fundamentals of the PA effect. This includes a thorough chronological review of advancements, experimental methodologies, and the intricacies of the source and detection of PA signals. The utilization of amplitude and frequency modulation, design of PA cells, pressure sensor-based signal detection, and quantification methods are explored in-depth, along with additional mechanisms induced by PA signals. The paper then delves into the versatile applications of photoacoustic imaging facilitated by functional nanomaterials. It investigates the influence of nanomaterial shape, size variation, and the role of composition, alloys, and hybrid materials in harnessing the potential of PA imaging. The paper culminates with an insightful discussion on the future scope of this field, focusing specifically on the potential applications of photoacoustic (PA) effect in the domain of biomedical imaging and nanomedicine. Finally, by providing the comprehensive overview, the current work provides a valuable resource underscoring the transformative potential of PA imaging technique in biomedical research and clinical practice.

* Corresponding author.
** Corresponding author.
*** Corresponding author.
E-mail addresses: siddhartha.g@srmap.edu.in (S. Ghosh), writoban.b@srmap.edu.in (W.B. Ball), sabyasachi.c@srmap.edu.in (S. Chakrabortty).
[1] These authors contributed equally to this review.

https://doi.org/10.1016/j.heliyon.2024.e34654
Received 22 January 2024; Received in revised form 8 July 2024; Accepted 14 July 2024
Available online 17 July 2024

1. Introduction

1.1. Nanotechnology and nanomaterials

Starting from first industrial revolution in mid-to-late eighteenth century, humanity has tried to understand the inner mechanisms of very big celestial objects like stars, planets, galaxies etc. to the very small, microscopic and then nano-scale objects.

Nano-scale objects and functional materials usher a new era of human civilization with a vast range of potential applications - from medical implants patrolling the arteries to the supercomputers with processing chips having transistors with gate lengths in the domain of 2–3 nm [(1a)]. This flexibility in the application of these miniature materials enabled dramatic changes in the technological world, encouraging innovation for the future. Nanotechnology (NT) makes use of nanomaterials (NMs), that have at least one external dimension of measure and a few nanometres of magnitude in that dimension.

Nanomaterials exhibit unique properties owing to their small size and can occur naturally or be engineered to meet specific requirements. Their dimensions, synthesis processes, and properties play a crucial role in their applications. These materials have gained widespread use in various industries and daily life, from drug delivery systems to sunscreens. Nanomaterials are intentionally engineered to take advantage of their small size, which often leads to distinct properties not observed in bulk materials. For instance, in the cosmetic industry, nanomaterials are utilized in sunscreens for their enhanced UV protection capabilities [(1b)]. Similarly, nanomaterials are employed in textiles to create stain-resistant clothing and find applications in many other everyday products. Reduced size of nanomaterials compared to bulk materials results in an increased surface area, leading to unusually high percentage to surface atoms leading to greater chemical reactivity and novel functional properties [(1a)]. The study of nanomaterial characteristics has gained momentum, with a focus on quantum effects and novel electric, magnetic, and optical behaviour. A wide variety of nanomaterials are commercially used today. For several decades, applications of nanomaterials have been prevalent in commercial products such as paints, textiles, coatings, and varnishes etc. Furthermore, nanocomposites are utilized in consumer goods like sports equipment, windows, and automobiles. Noteworthy examples include UV-blocking coatings on glass bottles that protect beverages from sunlight, as well as the use of titanium dioxide in self-cleaning windows, sunscreen formulations, and dental fillings [(1c)].

1.2. Advancement in nanotechnology and nanomaterials

As discussed previously, the influence of nanotechnology paved a path towards a spectrum of applications. This resulted in many nations investing in the research and development of nanotechnology. With the growing interest in research and development, nanotechnology industries started developing rapidly since 1980s resulting in commercialization of many related applications and the trend is constantly on the up [(1c)]. The demand for functional and structural materials for both the organic and the inorganic categories became prominent as their optical, electrical, electronic, magnetic, and catalytic properties were well understood. The production of cluster-assembled or nano-phase materials is dependent on the process of making small clusters that are separated and concatenated into a bulk material or solid/liquid compact. The following fundamental properties of nano-sized materials are predicted to advance in overlapping generations of numerous products which may include active nanostructures, passive nanostructures, molecular nano-systems, nanomedicine, food, agriculture, textile, nano sensors, nanoelectronics etc [(1b)].

1.3. Types of nanomaterials

NMs are extremely small in size, comparable to the size of molecular clusters. They have at least one dimension, which is of a

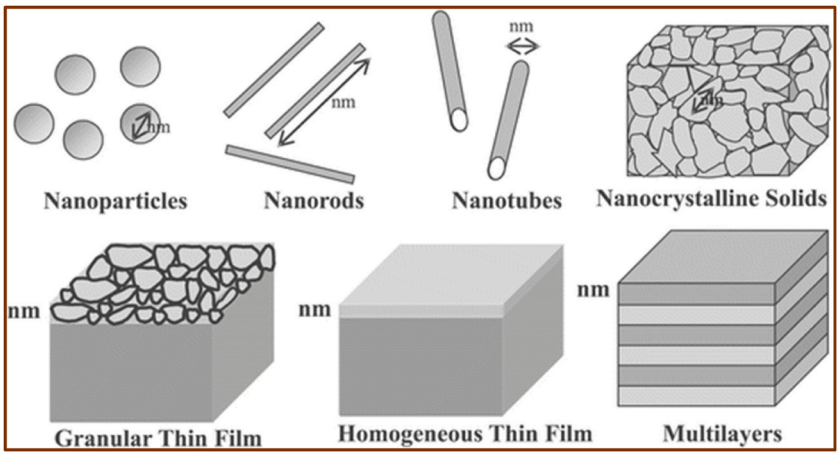

Fig. 1. Different types of NMs and nanocrystals are commonly found. Reprinted with permission. Copyright 2015 Capital Publishing company [(1b)].

magnitude ranging a few nanometres. These nano-structural materials are classified based upon the available dimensions along with their shape as illustrated in Fig. 1:

- Zero dimensional spheres and clusters
- One dimensional nanofiber, nanowires, surface films and nanorods
- Two Dimensional Plates, Strands and Networks
- Three-dimensional NMs like multi nanolayers and colloidal nanoparticles [(1d)]

These NMs exist as fused, single or agglomerates/aggregates which may be further classified depending upon their shapes and sizes Fig. 2. Some of the well-known shapes include the spherical, the cubic, the rod and the tubular. Other examples of NMs are dendrimers, nanotubes, fullerenes and quantum dots. All these different types of nanoparticles (NPs) serve various functions in the field of nanotechnology based upon their physical and chemical characteristics [(1c)]. For example, gold nanorods are good optical absorbers, while nanocages are capable of encapsulating drugs for targeted delivery. Similarly, the difference in constituent atoms of concerned NPs also have a significant impact on their chemical and physical properties. Carbon nanotubes, silver nanorods, fullerenes, silica based NMs have different properties enabling their utilization in various industries [(1e)].

Along with the classification based on shape, nanomaterials (NMs) are also characterized by their ultra-small size, typically measuring fewer than 50 nm [(1a)]. This size range allows the particles to exhibit unique properties and performance, leading to their further modulation and optimization for specific applications.

1.4. Functional properties of nanomaterials

The flexibility and controllability of nanomaterials in terms of synthesis and properties have sparked significant interest in research. Interestingly, non-linear optical properties of nanostructured semiconductors are identified to have several advantages. For example, quantum confinement effects shown by Q-particles may provide special use cases like luminescence in powdered silicon. Quantum dots made up of silicon-germanium can be utilized as optoelectronic devices in infrared radiation. In solar cells, window layers make use of nanostructured semiconductors [(1a)]. Porous coatings, dense parts, gas-tight materials are the applications of nanosized metallic powders which show properties like ductility along with the cold-welding properties of metal-metal bonding making them suitable for the electronic industry. The magnetic properties (coercive field and saturation magnetization) of single and multiple domain magnetic nanoparticles/nanocomposites demonstrate surprising differences. They can be utilized for targeted drug delivery, bio-imaging, ferrofluids, big data storage and spintronics [(1a)].

Metal nanostructures and mono colloids are being used as catalysts. These materials with pluri-metallic composition can be used as precursors for cortex-catalysis or heterogeneous catalysis due to their substantial advantages of selectivity, activity and lifetime in various chemical transformations, fuel cells and electrocatalysis. Nanoscale metal particles with chiral modifiers are found to be good at enantioselective catalysis [(1e)].

Metal oxide thin films with thickness in the ranges of few nm, have shown to be effective for their applications in gas sensors for detecting NO_x, CO, CH_4, CO_2 and hydrocarbons that are aromatic. These thin films have great sensitivity and enhanced selectivity. MnO_2 thin films are being used in rechargeable batteries for automobiles [(1d)]. Whereas Si thin films have gained popularity in thin-film solar cells due to their transparent contacts. Solar cells of dye sensitization require titanium oxide nano-structured films due

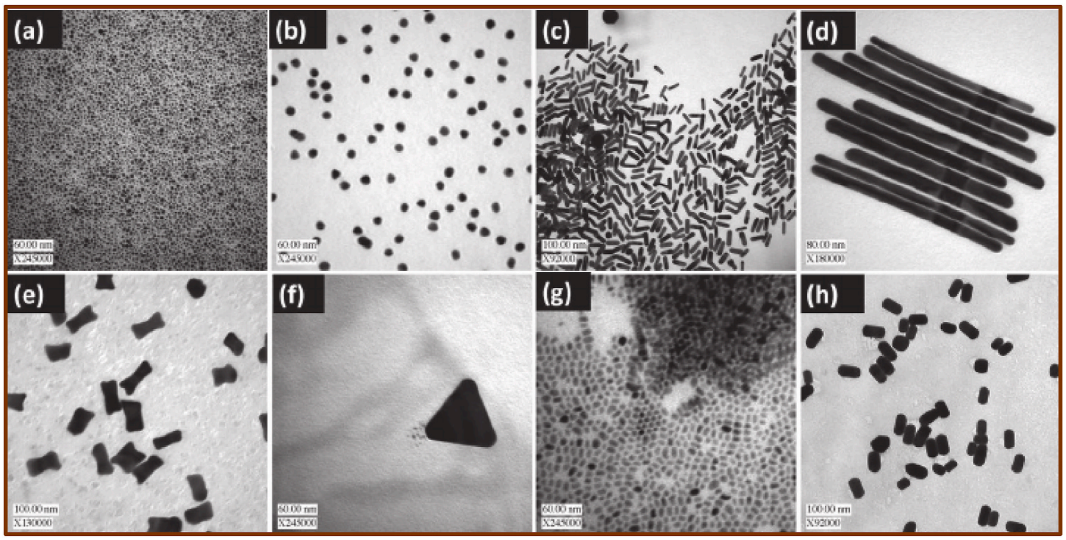

Fig. 2. Nanoparticles of different compositions. Reprinted with permission. Copyright 2011, Taylor & Francis [2].

to their advantages of good surface area and high transmission leading to good absorption [(1c)]. Polymer-based nanocomposites with a high dielectric-constant are useful raw materials to attain photonic bandgap structure due to the high percentage of inorganic particles.

1.5. Future of nanotechnology

Nanotechnology can provide valuable tools that can help us to deal with the future impending challenges like medical diagnosis, advanced manufacturing, self-healing structures, climate change etc [(1a)].

Nanotechnology-based devices having a size of tens to hundreds of nanometres can be utilized to serve the purpose of medical diagnosis by operating at the cellular level. In this field of research, NMs are already being used in diagnostic, targeted drug delivery and biomedical imaging applications [(1e)]. This gives our future generation a ray of hope in facilitating personalized medication which can be customized according to the genetic profile and specific disease type of the individual. In future, the medical diagnosis will have a dramatic improvement with nanoscale sensors and devices which may provide cost-effective and continuous monitoring of patients' health which may include early prediction of diseases and nanotools.

Similarly, nanotechnology and its applications also have a positive impact on manufacturing smaller, energy-efficient and more functional sensors. For example, cost-effective sensors having tiny features can help in printing large quantities of flexible plastic rolls [(1b)]. These advancements will lead to demand for portable, miniature, analytical devices with low cost.

Structural healing is one of the challenges where nanotechnology can play a pivotal role. Altering the structure of materials at the nanoscale will increase the functionality of materials and enhances their properties. Soon, various coatings and additives will be manufactured to enable materials to heal when worn or damaged [(3a)]. Also, dispersible NPs can migrate within the bulk of a material to fill any gaps or cracks that could appear [Fig. 3].

Nanotechnology (NT) will be also highly useful in tackling climate change and related challenges looming over sustaining our industrial civilization without harming the surrounding biosphere. Solar Panels, energy-efficient batteries, electric vehicles are some of the fastest-growing research areas [(1a)]. NMs provide more surface area, resulting in more reactions taking place in an energy generator. This in turn reduces the wastage of energy and helps the device to work efficiently [(1a)]. Forthcoming developments by the implementation of nanotechnology may include hybrid NMs that can produce energy from various external factors like variation in temperature, light with good conversion efficiency [(1a)].

2. Fundamentals of photoacoustic (PA)

The concept of photoacoustic (PA)/optoacoustic (OA) effect, is the conversion of high intensity modulating light (generally Laser) energy into sound emission. The idea was originally proposed by Alexander Graham Bell 150+ years ago (~1880). It deals with the measurement of absorbed light or electromagnetic radiation with the help of acoustic sensors. The phenomenon of the PA/OA effect was observed with the generation of sound waves as the result of absorption of light in a material [(3b)]. The intensity of the light or the electromagnetic radiation must keep varying constantly at regular intervals or as a single pulsed light or flash. Quantification of the PA effect is done by measuring the pressure changes or the sounds formed with devices such as microphones or sensors which are piezoelectric in nature [(3b)]. The variation of output with time, either in terms of voltage or current from the above discussed or piezoelectric sensor is the PA signal. The following generated signal helps in the determination of various functional material

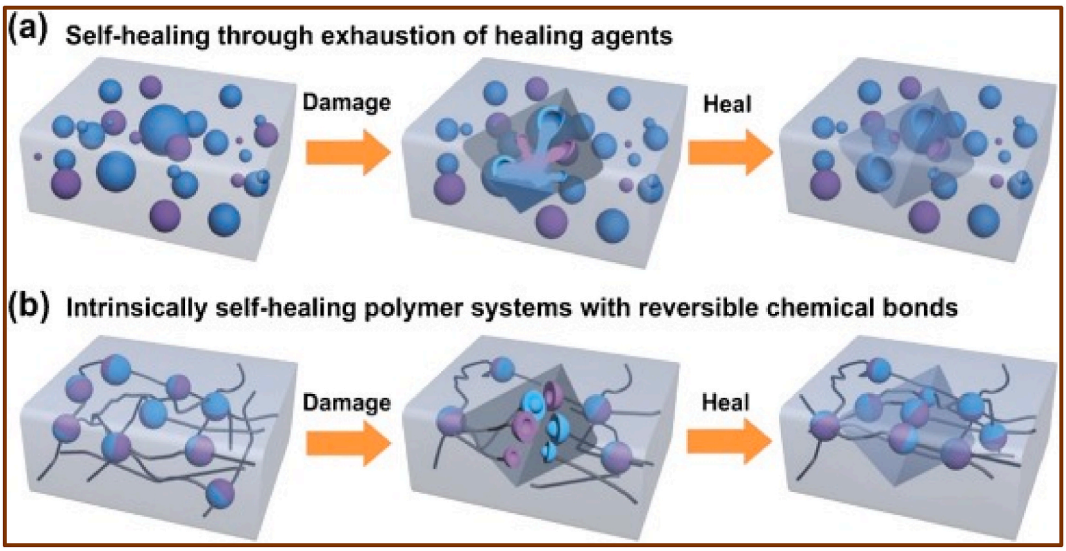

Fig. 3. Self-healing polymers. Reprinted with permission. Copyright 2020, Elsevier [(3a)].

properties of the samples of interest [(3c)]. The best example of the fore-mentioned process would be PA spectroscopy, in which the generated PA signal is used to infer the absorption of light either in transparent or opaque objects [(3c)]. One of the advantages of this method, when compared to other general procedures, include the flexibility and specificity utilizing a pulsed laser [(3c)].

PA measurements, serve as an essential tool for analysing and understanding photochemical reactions. This technique involves the measurement of thermal signals resulting from light absorption, allowing researchers to gain insights into various aspects of photochemical processes [(3b)]. Specifically, in the field of botany and the study of photosynthesis, PA measurements play a crucial role in investigating the energy transfer, photochemical efficiency, and overall dynamics of photosynthetic systems.

By employing PA measurements, researchers can examine the behaviour of plants and other photosynthetic organisms under different types of illuminations, study the impact of environmental degradation on photosynthetic processes, and gain a deeper understanding of the underlying mechanisms involved [(3c)]. The ability to quantify and analyze the thermal signals generated during photochemical reactions provides invaluable data for elucidating complex processes and advancing our knowledge in fields such as botany and photosynthesis research [(3c)]. Commonly, all the electromagnetic (EM) radiation ranging from microwave to radio and gamma radiation to X-rays can be exploited towards applications of the PA effect. But so far, most of the research and implementations include utilization of only visible, ultraviolet and infrared regions of the EM spectra [(3c)].

In detail, PA effect primarily involve the three steps outlined below [(3c)]:

- ➢ *Production of heat energy from the modulated radiation or absorbed pulse.*
- ➢ *Temperature variation in the region where the electromagnetic radiation was absorbed.*
- ➢ *Pressure changes due to the thermal expansion and contraction caused by the temperature variation.*

The change in pressure at the area of absorption of light propagates throughout the body of the sample and the same can be sensed by a sensor that is directly coupled to it. Generally, for solids and liquids, the variation in pressure is rather observed in the surrounding air due to the temperature gradients around the sample. This modulation of pressure gives rise to successive contraction and rarefaction in the gaseous medium surrounding the sample. This in effect initiate propagation of a longitudinal wave through the same gaseous medium, which we know as Sound wave. That is why this mechanism is termed as Photo-acoustic effect [5].

PA/OA effect can be utilized to precise and local information regarding any photochemical reaction, as the temperature and pressure gradient exponentially decay as we move away from the source [5].

Meanwhile, the changes in temperature and pressure are minuscule using normal light intensities, in the order of micro to millidegrees and nano to micro-bars, respectively [5].

Now, recording the PA spectrum of a sample is done by measuring the sound, utilizing the light at different wavelengths. The short pulse and rapidly modulated radiation are used as inquisitive energy, having the capability of detecting the ultrasound [5]. This ultrasound is created by photon absorption and thermo-elastic expansion. The spectrum which is produced can enable the identification of absorbing components in the sample of interest Fig. 4.

Previously, PA has seen its implementation in studying solids, liquids and gases [5]. The study of PA has gained the attention of researchers in various fields such as engineering [6], physics [7] and medicine [8] due to their wide range of applications. The potential to give functional, kinetic, molecular and structural details employing endogenous contrast agents such as melanin, haemoglobin, lipids and water or a range of different contrast agents which are exogenous or two of them put together, demonstrated the broad variety of applications. This includes the applications in the fields of spectroscopy, biosensors and other miniature PA instruments in the electronics industry. Along with the same, few contrast agents were tabulated in Table-1, which were also discussed consecutively.

The progress of PA research across various fields has contributed to its increasing significance in medical imaging. One such example includes providing great contrast of blood vessels. In addition to this, PA is also efficient in imaging blood oxygen saturation (functional imaging) as well as providing molecular imaging of cells, tissues, and organs at greater depth and resolution. This advantage is attributed to the use of ultrasound energy in PA imaging, which overcomes the limitations of light energy such as

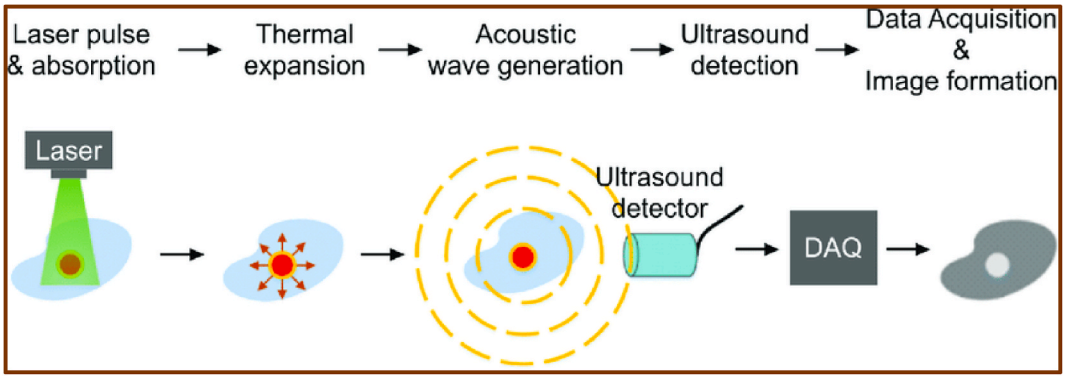

Fig. 4. PA signal generation, acquisition and detection. Reprinted with permission. Copyright 2019, Elsevier [4].

Table 1
Contrast agents and its applications.

Contrast Agent	Type	Advantages	Disadvantages	Applications
Gold Nanorods	Inorganic	Good penetration depth	Limited absorption efficiency, High cost	Brain tumor imaging, Photothermal therapy
Silver Nanoparticles	Inorganic	Good tissue transmission windows		Thermo-plasmonic, Photothermal therapy, Photothermal imaging, PA imaging
Melanin Nanoparticles	Organic	Dual-labeling agents (MRI and PA imaging), Biocompatible		Stem cell labeling, Tumor detection
Copper Sulfide Nanoparticles	Inorganic	Deep tissue imaging, Photothermal ablation of cancer cells		PA tomography
Nickel Dithiolene Nanoparticles	Organic	Sharp and strong absorption peak for deep tissue imaging		PA imaging
Perylene-based Organic Nanoparticles	Organic	Improved permeability and retention for brain tumor imaging		PA imaging of brain tumors
Conjugated Polymer Nanoparticles	Organic	High non-radiative quantum yield, strong near-infrared absorption, good photostability		PA vascular imaging, Photothermal therapy

scattering and attenuation. The promising features of PA techniques transformed it into an important biomedical imaging method providing the gains of the acoustic depth penetration and a good optical resolution. Also, the spatial distribution of the optical absorption is better even at the deepest tissue level along with greater penetration depths and better resolution, than that of traditional optical imaging methods [9]. In the successive section, the advancements of PA as of now have been explained in detail.

2.1. Chronological advancements

PA effect was originally observed with an experiment revealing the photosensitivity of selenium. The outcome of the experiment showed that when an electric current was passed through a crystalline selenium bar, its resistance was found to be less compared to an identical selenium bar kept in the dark [10].

The results of this study ensued further investigation explaining the relationship between the changing resistance and the irradiation as follows:

- Understanding the relation between changing resistance and luminous rays
- Comparing the changes in resistance with respect to various light sources
- Determining the potential of light energy in producing electricity
- Examining the electrical conductivity of selenium in the dark

Later, the production of sound with the help of light energy was demonstrated. Similar studies revealed the remarkable properties of selenium and several other materials like gold, platinum, antimony, silver, iron, brass, steel, lead, zinc, and copper, to name a few [11]. Similar studies have shown the modulation of sound waves directly in response to the amplitude of electricity. The electric current that was modulated and sent through the telegraphic wires was utilized to transmit sound. In this case, the selenium wire could convert the modulated light into sound waves [12].

Following the observations which are discussed above, further experimentation has shown that the special properties of specific substances could also be observed in the liquid and gaseous forms of matter [13]. In the same manner, the action and effect upon the gaseous matter because of an intermittent beam of radiant energy were described [14]. Additionally, many studies and research work found that a variety of materials, under identical conditions, exhibit similar sonorous property irrespective of the state of the matters being solid, liquid or gas [15]. These fundamental observations led to the discovery of a device called spectrophone [16]. The functioning of the device exploits the ability of light to generate sound. An object placed in the middle absorbs the energy that is focussed from a beam of light followed by a thermal expansion which is time modulated and can be detected with the help of a simple stethoscope.

A waveguide ring resonator utilizes light in order to detect the sounds. The light is generally coupled by using a waveguide leading into a micro ring. When the wavelength is comparable to the ring circumference, waveguide dimensions get distorted, altering the observed resonance spectrum. Rayleigh reported sound wave generation by the simple effect of intermittent radiation on thin plates of a wide range of substances [17].

Parallel investigations on a wide range of materials demonstrated that the production of sound was not a cause of the vibrating disc but was actually a result of contraction and expansion of the air along with the disk which was intermittently heated [18,19]. Meanwhile, other research work [20] also found similar results following periodical heating and cooling, resulting in contraction and expansion, respectively. Experimentation on thermal currents was presented in [21], which reported noteworthy results. The study highlighted that the rate of heating, as well as the contraction and expansion, vary almost directly in response to the decrease/increase of current, although these variations are very small. Later, experimental works [22] were conducted to explore the transmission of speech signals using light as a medium, aiming to investigate the potential of optical communication for speech transmission.

In a seminal study, light was captured from a point source utilizing a lens with a focal length of 1 m. The resultant image was

projected onto a concave mirror, which was subsequently affixed to a gramophone recorder. By inducing divergence, the light passed through an identical lens and was then projected onto a remote station. Both lenses were equipped with grids placed in their respective paths. Notably, the image from the first grid was superimposed onto the second grid using a concave mirror. Intriguingly, the oscillatory behaviour resulting from sound vibrations was observed in the latter grid. Research work was done building upon Tyndall-Rontgen optic-acoustic effect. It was illustrated that when the radiation of absorbing gases and vapours were exposed to thermal radiation with periodic interruption, a corresponding cooling and heating of gases occurred. This, in turn, resulted in fluctuations in the periodic pressure, making way for sound emission and the earlier known optic-acoustic effect was commonly referred to as the Tyndall-Rontgen effect at that time.

Further studies presented some of the physical methods to measure the concentrations of certain vapours and gases in the atmospheric air. The methods described in the study are limited to compounds like carbon dioxide, methane and carbon monoxide having good characteristic absorption bands present in the infrared [23].

In extension to the existing research, an infrared gas analyser was constructed to measure the trace of gases with the help of absorption of the emitted infrared source of light by taking an air sample. This gas analyser worked with the help of microphone detectors and has two cells, one containing the sample of interest, while the other cell has the concentration of reference gases. A coupled chamber was found to be separated by a membrane capacitor and the infrared sources were made to periodically interrupt by means of a rotating disk having acoustic signals generated. These acoustic signals were calibrated as a differential signal from the microphone [24].

The experiments related to optoacoustic properties, implementations and their advantages gained prominence with time. Along with this, the name of the technique with reference to the "spectroscope" was eventually changed to "optoacoustic analysis" [25] which was widely used for the analysis of gases. The timeline chart of the following section is provided in "Fig. 5."

2.2. Methods and experimentation

The concept of PA imaging encompasses a broad spectrum of choices and aspects that are contingent upon the characteristics of the absorbed radiation. Selecting a particular scheme for a problem statement depends largely upon the sample of interest, operational flexibility and many other requirements. Typically, for solids, liquids and gases, parameters like temperature and pressure may vary significantly.

In the same way, there are also considerable variations within the same state of matter. For example, the analysis of samples in solid-state includes the measurement of pressure which is generated either directly with the help of a piezoelectric sensor for a pulsed regime or, a gas in contact can be used with the help of a microphone.

In the gas phase, the measurement in diffused direction of the acoustic wave is unavoidable. In this case, it is impossible to have direct contact with the sample. This phenomenon can also be seen in the case of powders, greases, or gels.

Moreover, if deployment of piezo based pressure sensors is non-suitable due to the nature of experiment/higher temperature, PA signal measurement through non-contact methods have an advantage [Fig. 6].

Also, the temporal and spatial gradient of the refractive index can be made by monitoring the deflection from a probe beam in a transparent sample, otherwise, above the surface of the sample. In situations where non-contact methodologies are utilized, slight deformations or surface reflectivity can also be analyzed by means of a probe beam. Changes in thermal radiation from the surface of the sample can be observed by an infrared detector. The following technique employs Stefan-Boltzmann law. Other such methods are

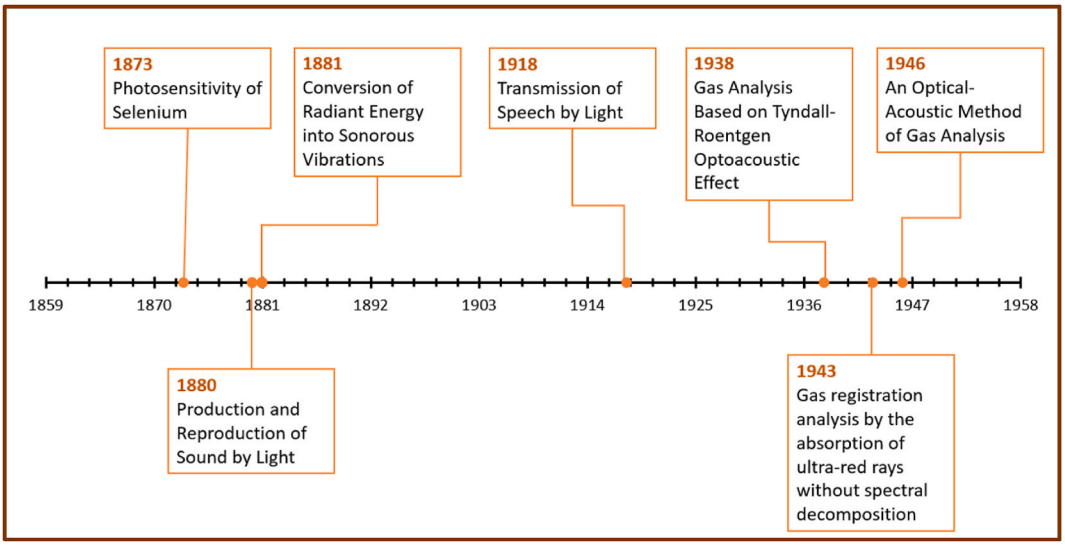

Fig. 5. Timeline of PA related experimentation.

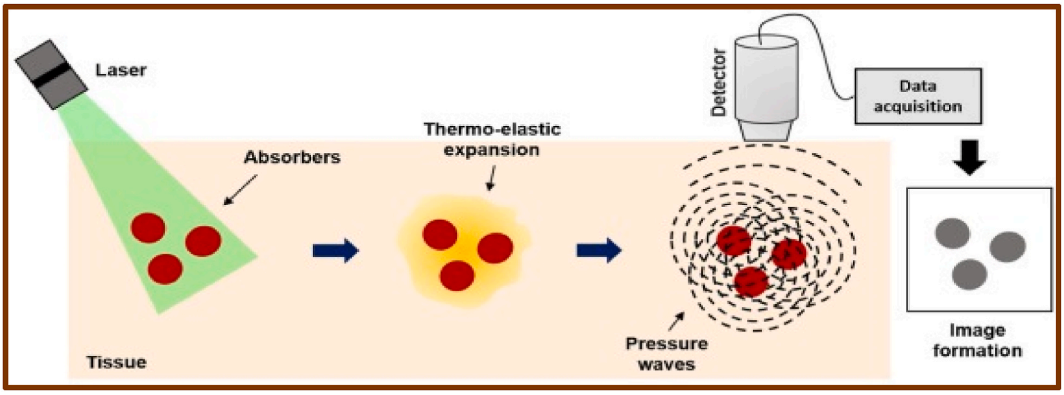

Fig. 6. Illustration of non-contact methods of PA imaging. Reprinted with permission. Copyright 2020, Elsevier [26].

pyroelectric detection in case of analysing thin films, interferometric methods and thermal lensing.

In the case of weakly absorbing liquids, the general arrangement has a tunable pulsed laser that can direct a beam through the PA cell containing the sample of interest. The acoustic waves which are generated will be detected by a transducer that has less response time. Generally, the initial raise or peak of the acoustic signal is observed and utilized for further processing. The variation in pulse to the pulse of laser power is described for the normalization of the piezoelectric signal.

Another important aspect of the analysis is the measurement of strongly absorbing or opaque liquids. An optothermal window, or simply a PA cell was made for this application. It contains an uncoated window and lead zirconate titanate (PZT) transducer at the bottom. A laser beam passes without any obstruction through the window and a droplet of the sample gets deposited on the other end of the disc. The heat which is generated in the process, diffuses into the above-said disc and ultimately expands. The transducer then records the induced stress. Unlike the traditional transmission spectroscopy, in which the thickness of the cell is a restriction in dealing with highly absorbing samples, the magnitude of the opto/photo-thermal window depends upon the product of thermal diffusion length and absorption coefficient. Whereas the latter can also be adjusted with the help of modulating frequency.

In gaseous phase measurements, the typical setup involves a narrow-width tunable laser or a broadband radiation source, accompanied by optical filters. Pulsed or amplitude-modulated radiation is commonly transmitted through the PA cell. The acoustic sensor used is usually a condenser microphone or a commercial electret microphone, both of which are user-friendly and suitable for studying trace gases with low absorptions. Detection thresholds are commonly determined based on ambient noise, molecules at the cell wall and window heating, rather than microphone sensitivity or electrical noise. However, fluctuations in radiation intensity, amplifier noise, and microphone sensitivity are employed to measure and assess sensitivity.

The impact of microphone sensitivity is generally minimal, but temperature dependencies should be considered in special cases. When modulated radiation is employed, the microphone signal is sent to an amplifier synchronized with the modulation frequency. Consequently, for weakly absorbing media, the absorbed power is directly proportional to the microphone signal's amplitude. Additionally, the average radiation power is recorded using a power meter for normalization. If pulsed radiation is utilized, the microphone's bandwidth may not be sufficient to resolve the temporal structure of the generated pulses.

Microphones can typically be employed for laser pulses of nanoseconds since the length of a single acoustic pulse is determined by the transit time of the acoustic wave transversing the beam radius. The PA amplitudes are obtained by dividing the peaks of the microphone signal by the corresponding laser pulse energy, which is recorded using a pyroelectric detector. Taking the mean of all pulses enhances the signal-to-noise ratio.

Another approach for pulsed radiation involves using an acoustic resonator with a high Q-factor as a gas cell and capturing signals in the time domain using a microphone. The analysis of PA signal amplitudes is performed after Fourier transforming the signals into the frequency domain, allowing observation of PA frequency spectra and excited cell resonances.

Calibration of the PA system is crucial for many applications, as the PA signal depends on various factors with limited accuracy. A general calibration can be achieved using a reference sample with a known absorption. While gaseous mixtures can be calibrated during experimentation, the calibration process becomes more intricate with structured morphological samples such as tissues, powders, and gels. Obtaining quantitative data in such instances is challenging, leading to reliance on qualitative analysis to extrapolate information when spectroscopic techniques fail due to strong scattering or opaqueness of the sample.

It is important to note that numerous variations and modifications of the schemes can be devised, incorporating other conventional methods like Fourier transforms or chromatography techniques. In the next section, we will briefly discuss additional aspects of detecting PA spectrometer components.

3. Source and detection of PA signal

In many of the commercial applications of the PA, incandescent lamps are being used as light sources along with light-emitting diodes, interferometers, or filters. In compact gas sensors, the source of modulated radiation consists of devices equipped with a small light bulb modulated by direct current or a chopper. Appropriate filters are used to avoid interference from other species present

["Fig. 7"].

However, it is important to note that the generated PA signal is proportional to both the incident and absorbed radiation power. While the previous paragraph focused on the generation of PA signal, it is worth mentioning that powerful radiation sources such as lasers offer significant advantages in terms of spectral brightness. They play a crucial role in achieving excellent detection selectivity and sensitivity in various spectroscopic applications. Depending on the spectral range, lasers should be carefully selected. For instance, in the visible and UV ranges of the spectrum, commonly used options include dye lasers and excimer lasers. Whereas, in fundamental or mid - Infrared (IR) regions, carbon monoxide or carbon dioxide lasers have greater prominence. Similarly, for monitoring overtones and interpreting combination bands in molecular absorptions, near IR diode lasers have a greater advantage.

Narrow band and widely tunable solid-state laser devices are used in the mid-IR region in order to access the fundamental absorptions (stronger). Recent and budding developments of mid- IR tunable lasers have a long way to go for future applications.

3.1. Amplitude & frequency modulation

Modulation schemes can be broadly categorized into two main types: modulating the absorption of the sample and modulating the incident radiation. The commonly used method in the second category is Amplitude Modulation (AM). AM of continuous radiation is achieved using acousto-optic or electro-optic modulators, choppers, or modulated source emission. Pulsed excitation or current modulation is employed to modulate the source emission.

On the other hand, Wavelength Modulation (WM) or Frequency Modulation (FM) can yield more valuable results compared to AM by eliminating the continuous background caused by absorption independent of wavelength. An illustrative example is window heating, which is particularly efficient for absorbers with small linewidth and simplified performance. This type of modulation, when combined with radiation sources, allows for rapid tuning within a few wavenumbers. Pulsed excitation is commonly used for liquid samples and is gaining popularity in applications involving gaseous samples due to advantages like time-gating and acoustic resonance excitation.

In spectroscopic analysis of complex gas mixtures, enhancing selectivity and sensitivity is paramount. Modulating the sample's absorption characteristics offers a powerful approach. The Zeeman and Stark effects exploit the interaction between an applied modulated magnetic or electric field and a molecule's inherent properties, such as the permanent electric dipole moment. This targeted interaction leads to significant changes in absorption for specific molecules (e.g., NO, NH_3) while minimally affecting interfering species (e.g., CO, H_2O). This effectively "filters" the desired molecular signal from the background. Furthermore, combining absorption modulation with light source intensity modulation (amplitude modulation) provides an additional layer of selectivity and sensitivity improvement, particularly valuable for multicomponent samples. This combined strategy proves highly effective in scenarios like detecting trace ammonia (NH_3) amidst carbon monoxide (CO) and water vapor (H_2O). Through these modulation techniques, researchers gain a powerful tool for achieving superior selectivity and sensitivity in complex gas analysis.

3.2. Design and utilization of PA cells

A PA cell serves as a container for storing the sample of interest. As an attachment to the same, a microphone is used to detect and capture the generation of acoustic waves. This can be better understood through the visual representation provided in Fig. 8A simple PA cell design characterizes a pivotal point in case of mitigating background noise and finally in limiting the sensitivity of detection. In some of the instances, in the applications related to trace-gas, most of the cell configurations have been used like non-resonant cells, acoustically resonant cells, single and multi-pass cells etc. Non-resonant cells generally have small volumes and are mostly used for analysis on solid samples having a modulated excitation. Similarly, such type of cells has also seen their utilization while working with gaseous and liquid samples with pulsed laser excitations.

The choice and optimization of resonant modes in cell design are essential to maximize the detection sensitivity in gas monitoring. By precisely engineering the cell dimensions, material properties, and resonant frequencies, it is possible to create a resonant cell that effectively captures and amplifies the acoustic signals generated by the absorbed radiation. This strategic design approach ensures the efficient conversion of optical energy into acoustic waves, leading to enhanced detection capabilities and improved gas sensitivity.

Therefore, understanding the significance of cell design and its impact on detection sensitivity is crucial in developing high-performance gas monitoring systems. By harnessing the power of resonant modes such as azimuthal, longitudinal, and Helmholtz resonances, parameters such as the interaction between the excitation source, the sample, and the resonant cell can be optimized,

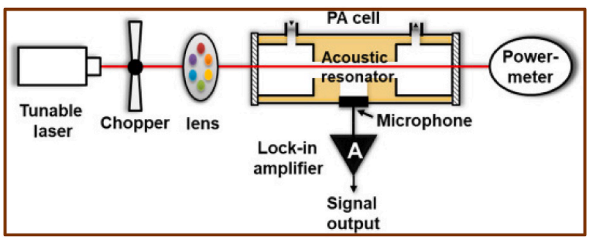

Fig. 7. Industrial PA application set-up. Reprinted with permission. Copyright 2020, Elsevier [27].

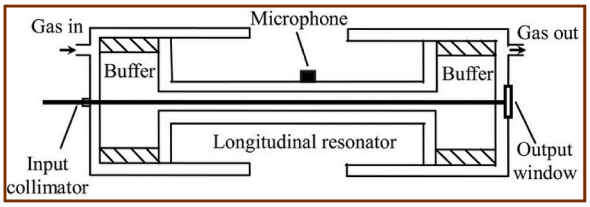

Fig. 8. Structure of PA cell. Reprinted with permission. Copyright 2013, Springer [28].

ultimately improving the accuracy and reliability of gas detection and analysis.

Resonant cells, commonly utilized for gas monitoring, employ modulated excitation and operate based on various resonances, including azimuthal, longitudinal, and Helmholtz resonances.

- **Azimuthal resonances** involve the circular motion of the gas molecules within the cell, resulting in a well-defined resonance frequency. This type of resonance is particularly useful for samples with cylindrical symmetry, such as gases confined in cylindrical cells. By exciting the azimuthal mode of vibration, the PA signal can be optimized, leading to improved detection limits and accuracy.
- **Longitudinal resonances**, on the other hand, pertain to the back-and-forth motion of the gas molecules along the axis of the cell. This type of resonance is commonly exploited in cells with a rectangular or cylindrical geometry. By exciting the longitudinal mode, the PA signal can be enhanced, enabling better detection of species with high absorption coefficients or low concentrations.
- **Helmholtz resonances** are based on the resonance of the gas within a cavity formed by two or more parallel surfaces. These resonances depend on the dimensions and geometry of the cell, and they can be employed to amplify the PA signal. By tuning the dimensions of the cell to match the desired Helmholtz resonance frequency, improved detection sensitivity can be achieved.

By leveraging the advantageous features of these resonances and carefully designing the resonant cell, PA spectroscopy can provide enhanced performance, improved detection limits, and better accuracy in gas monitoring applications.

Enhancing the signal using a high Q-factor offers several advantages. The resonance frequencies typically fall within the kilohertz range, resulting in resonant widths measured in multiples of hertz. Designing the gas handling system to position inlets and outlets at pressure nodes of acoustic resonance allows for more accurate flow rate quantification without increasing noise levels.

In the context of PA spectroscopy, specialized cell designs are developed for specific applications. For example, window-less cells equipped with acoustic baffles effectively reduce the effects of heat and ambient noise, making them suitable for analysing low volatile liquid samples.

Furthermore, PA spectroscopy enhanced by quartz components offers improved performance when working in open-air environments without requiring a traditional cell. This enhancement is achieved through the use of microtubes. Quartz, being a crystalline form of silica, possesses several advantageous properties that contribute to its superior performance in PA spectroscopy.

1. Firstly, quartz exhibits high optical transparency across a broad range of wavelengths, including UV, visible, and IR regions. This exceptional transparency allows for efficient transmission of modulated radiation used in PA spectroscopy. As a result, a larger portion of the incident radiation reaches the sample, maximizing the excitation efficiency and signal strength. The increased optical transmission of quartz enhances the sensitivity and accuracy of PA measurements.
2. Secondly, quartz demonstrates low acoustic absorption, minimizing the attenuation of acoustic waves generated during PA excitation. This characteristic ensures efficient transfer of acoustic energy from the sample to the surrounding medium, leading to stronger and more detectable PA signals. The reduced acoustic losses in quartz components contribute to improved detection limits and enhanced signal-to-noise ratios in PA spectroscopy.
3. Furthermore, quartz exhibits excellent thermal stability and low thermal expansion coefficients. These properties make it well-suited for PA spectroscopy in open-air environments where temperature variations are likely. The thermal stability of quartz components ensures consistent performance and reliable measurements, even under challenging conditions. Additionally, its low thermal expansion coefficients mitigate the impact of temperature fluctuations, preserving the dimensional integrity of the microtubes used in open-air setups.
4. Lastly, quartz is chemically inert and highly resistant to corrosion. This chemical stability enables the use of quartz microtubes with a wide range of samples, including reactive or corrosive substances. The compatibility of quartz with different sample types makes it a versatile choice for PA spectroscopy applications, expanding its utility in various research and industrial settings.

In conclusion, PA spectroscopy enhanced by quartz components offers improved performance in open-air environments through the utilization of microtubes. The exceptional optical transparency, low acoustic absorption, thermal stability, and chemical resistance of quartz contribute to enhanced sensitivity, improved detection limits, and reliable measurements. These advantages position quartz as a preferred material for PA spectroscopy, enabling advanced analyses in diverse fields such as environmental monitoring, gas sensing, and biomedical research.

3.3. Detection of PA signal using pressure sensors

As mentioned in the previous section, the generation of any kind of disturbances in the sample can be sensed by employing a pressure sensor. When the sample that needs to be analyzed is a solid or liquid, piezoelectric devices such as PZT, quartz crystals or $LiNbO_3$ have been widely operated. These devices have greater responsivity in the order of Volts/Bar while others can also have lower responsivity such as polyvinylidene-difluoride foils. These sensors are better known for their fast responses and are therefore usually adapted for usage in pulsed PA applications.

In the studies related to the gas phase, commercial microphones have gained prominence. These include Knowles or Sennheiser models, miniature electret microphones and condenser microphones. Typically, frequency has an almost little or negligible effect on responsivity. All these microphones have their own functionalities and can help in modulation frequencies of the range of 100 Hz to 1 kHz. In the instance of pulsed applications, the dependency between bandwidth and responsivity along with the manifestation of external noise results in a decline in signal-to-noise ratio for large bandwidths.

Therefore, miniature electret microphones are commonly good instruments for detection in that case. Enhancement of detecting sensitivity could be done by adding up the signals from several microphones. In such an arrangement the signal improves with the total number of microphones utilized. Along with the following, the random noise from the microphone increases proportionally to the square root of their count. Since electret microphones are small and cheap, many of such microphones can be used in a well-designed compact structure. Additional development of sensitivity is projected by concatenating it with an electrical filter by which the components with low frequency can be cut down of the signal. These components have less or negligible impact on the signal-to-noise ratio in comparison with the components with high frequencies. Another noteworthy point includes the adaption of microphone frequency response so that the full operation of the microphone could be exploited to sense all the frequency contributions except the components contributing to the noise.

While the PA spectroscopy enhanced by quartz scheme employs the tuning fork as the device to sense, other methods like PA spectroscopy enhanced by cantilever relies upon the acoustic wave which is generated in a cell using an interferometer.

In case of a necessity for non-contact detection, thermal sensing, refractive sensing and both Photothermal and PA deflection can be used. These techniques make use of a probe beam and pump beam in either a transverse or collinear arrangement. In comparison to the commonly used PA techniques by employing the pressure sensors like the piezoelectric, the above schemes also provide a comparable sensitivity. But these techniques need a complicated arrangement and stringent calibration.

3.4. Quantification of PA signal strength

The application of the PA effect involves various methods of quantification, depending on whether the sample being studied is in a condensed phase or a gaseous state. In PA measurements, pressure variations are typically measured in the immediate vicinity of the sample. The chosen timescale for studying chronological variability usually ranges from milliseconds to a sub-second scale.

In many cases, a technique called continuous modulation or chopping is used, where light is modulated at a specific frequency. The resulting PA signal can then be analyzed using a lock-in amplifier to interpret its quadrature, in-phase (or phase and amplitude) components.

When measuring pressure in the condensed phase, piezoelectric sensors are commonly employed. These sensors are often coupled or inserted into the sample itself. The timescale for such measurements generally falls within the range of microseconds to nanoseconds.

The PA signal obtained from different pressure sensors is influenced by several factors. These factors include the properties and physical characteristics of the system, the mechanism used to generate the PA signal, the specific characteristics of the material absorbing the light, the dynamics related to the relaxation of the excited state, the modulated frequency, the pulse-related information of the radiation used, and the properties of the sensor itself.

Based on these factors, signals can be separated and analyzed according to their system mechanisms, the time dependence of heat evolution, the rate of change of volume, or the PA signal with respect to time.

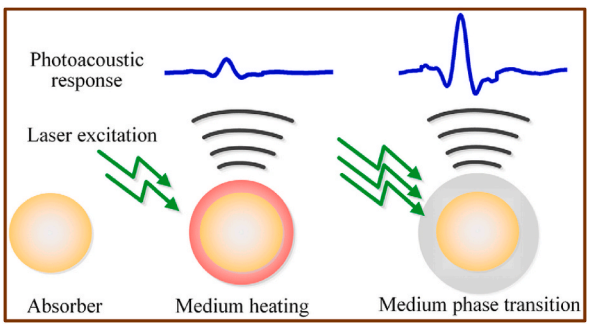

Fig. 9. Image illustrating the PA signal-induced thermal expansion. Reprinted with permission. Copyright 2018, SPIE [29].

3.5. Additional mechanisms induced by PA signal

Though the implementation of the PA technique has gained a lot of momentum utilizing the latest advancements in nanotechnology, other methods and mechanisms superimposed on the PA effect could be worked out in yielding better results. Studies on the following techniques will have a significant contribution to the PA signal and improvement of the photothermal mechanism. These methods which are allied to the following field are collectively called photochemical reactions. The key steps in the following processes include

- Variations in the material balance of the sample or the change in surroundings (air) of the sample [Fig. 9].
- Alteration in the molecular structure causing changes in the volume of the substance [Fig. 10]

Analysis and emphasis on the following reactions or processes will help in understanding the interference of light and the relation between pressure and thermal fluctuations. Some of the examples of the following contain analysis on oxygen consumption because of photo-oxidation of rubrene [31]. Correspondingly, studies were done to understand the modifications that occurred in fullerene-porphyrin systems utilizing PA and photothermal techniques [32]. In contrast to the examples specified above, one of the most interesting phenomena comprises photosynthesis and many other biological reactions.

Photosynthesis as a photo-chemical reaction also follows the fore-mentioned two steps. The operation of the first step can be evidently observed in the plant leaf. In this step, the oxygen evolution which is induced by the sunlight causes a significant pressure change in the air in turn leading to a PA signal. This is comparable to a general photothermal mechanism in terms of magnitude; hence, the same process can also be named a 'photo baric' reaction. The second step which is illustrated above [Fig. 10] can be realized in the reaction centres of photosynthesis, as the induced light initiates an electron transfer process creating a micro electrostriction effect affecting the molecular volume. This process also induces a wave of pressure propagating in the macroscopic medium. A similar process can also be observed in (Bacteriorhodopsin) proton pump, where the molecular volume change is a result of confirmational changes that take place in this protein with good light absorption.

PA measurements have a greater role to play in measuring the photosynthetic activities, photochemistry and exchange of gases [33]. Likewise, the non-destructive nature of PA spectroscopy has seen its implementation in studying the absorption spectral features of opaque solids like surfaces, solids and biological specimens such as microorganisms, cells and tissues [34]. In order to achieve more benefit out of the PA procedures, a computer-controlled pulse modulation system was designed which was distinct in contrast with conventional analysis in the frequency domain [35].

4. Nanoparticles and applications of PA effect

PA techniques offer diverse applications in different fields, including spectroscopy, medical imaging, energy conversion, and material analysis. Their ability to provide detailed information about absorption spectra, energy storage, and material properties makes them valuable tools in scientific research and technological advancements.

Considering only the applications of the photothermal process, the acoustic signal itself can quantify the absorption spectrum, particularly for transparent samples with low light absorption. Compared to general absorption spectroscopy, which relies on the variation of light intensities before and after passing through a sample, PA techniques provide more detailed information. However, in PA spectroscopy, the signal is related to both light intensity and light absorption. The ratio of the signal spectrum to the light intensity spectrum can provide a relative percentage that can be calibrated to obtain absolute values. This allows for the analysis of small

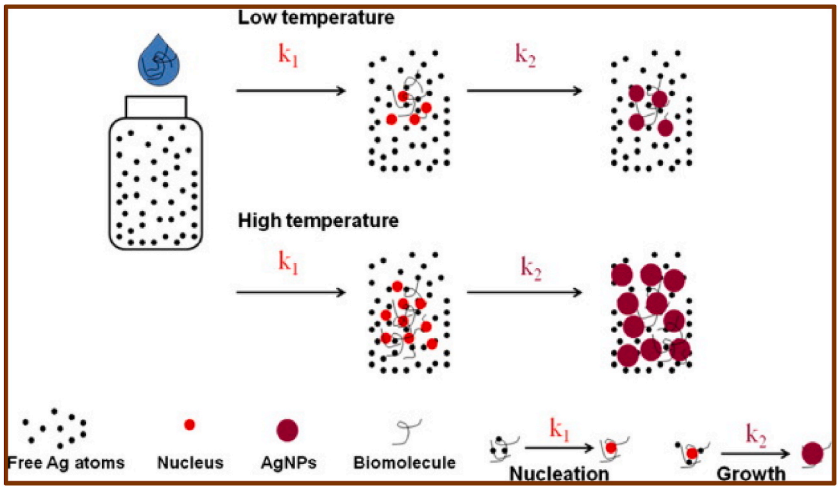

Fig. 10. Temperature effect on the size of silver nanoparticles. Reprinted with permission. Copyright 2020, Elsevier [30].

quantities and sample concentrations.

The combination of ultrasound and optical techniques has significant potential in medical applications, and low-cost PA imaging techniques have gained attention in recent years [36]. PA spectroscopy can also be applied to opaque samples. In the case of studying opaque samples, a sensor is typically positioned close to the gaseous phase near the sample, and the resulting PA signal propagates from the absorption zone towards the surface. An important parameter influencing the formation of the acoustic signal is the thermal diffusion length, which varies depending on the material and modulation frequency. The thermal diffusion length is typically in the micrometer range and aids in determining the absorption spectrum.

Surface analysis separate from the bulk of the material can be achieved by leveraging research in surface chemistry, allowing for utilization of features such as absorption losses [37,38]. Additionally, altering the wavelength and modulation frequency of the probing radiation enables variation in the probed depth, facilitating depth profiling [39,40]. Depth-dependent optical absorption coefficients can be calculated from the PA frequency responses, proving to be effective. PA imaging has also found applications in the detection of inhomogeneities [41,42] within a sample, aiding in the understanding of material properties through PA signals.

Another notable application of the PA effect lies in approximating the amount of energy stored and converted [43] during different stages of photochemical reactions, with a particular emphasis on photosynthesis [44]. After light absorption, photochemical and photophysical processes occur, storing light energy as chemical energy, which subsequently evolves as heat energy, resulting in a detectable PA signal that provides quantitative information about energy storage. For transient species, this process involves measuring the signal in an appropriate timescale. This mechanism plays a significant role in various applications, such as studying energy conversion efficiency [45,46] in solar cells and identifying suitable materials for their manufacturing [47].

Currently, PA techniques have been implemented in the quantitative measurement and analysis of nanomaterials (NMs), nanoparticles (NPs) and macromolecules, including proteins [48]. Various material properties, such as photothermal treatment, absorption, scattering, bioimaging, PA response, aggregation, and treatment, have been analyzed using PA and related techniques. A more detailed review of these mechanisms is provided in the next part of this review, which describes NPs and NMs of different shapes, sizes, and types.

4.1. Dependence on shape

There are various types of NPs that are commonly discussed in the field of nanotechnology. In this section, we will explore some of these NPs, characterized by their shapes as shown in Fig. 11. Different shapes of NPs exhibit distinct advantages and play important roles in various fields. In the area of exogenous contrast agents for biomedical PA applications, noble metal NPs, particularly silver and gold, have been extensively studied. These metals possess good tissue transmission windows in the visible to near-infrared bands. Geometrically diverse shapes of silver and gold NPs, such as spherical core-shell structures, nanorods, and nanocages, hold promise for applications in thermo-plasmonic, photothermal therapy, photothermal imaging, and PA imaging. Simulations of PA responses in a water medium have been performed for core-shell and gold NPs, using finite element methods to analyze the effects of laser pulse excitation on temperature distribution and PA pressure. Optimization of dimensions, such as the thickness of the gold-silica shell and the core diameter, has been carried out to improve PA conversion efficiency. Moreover, studies have explored the impact of shell

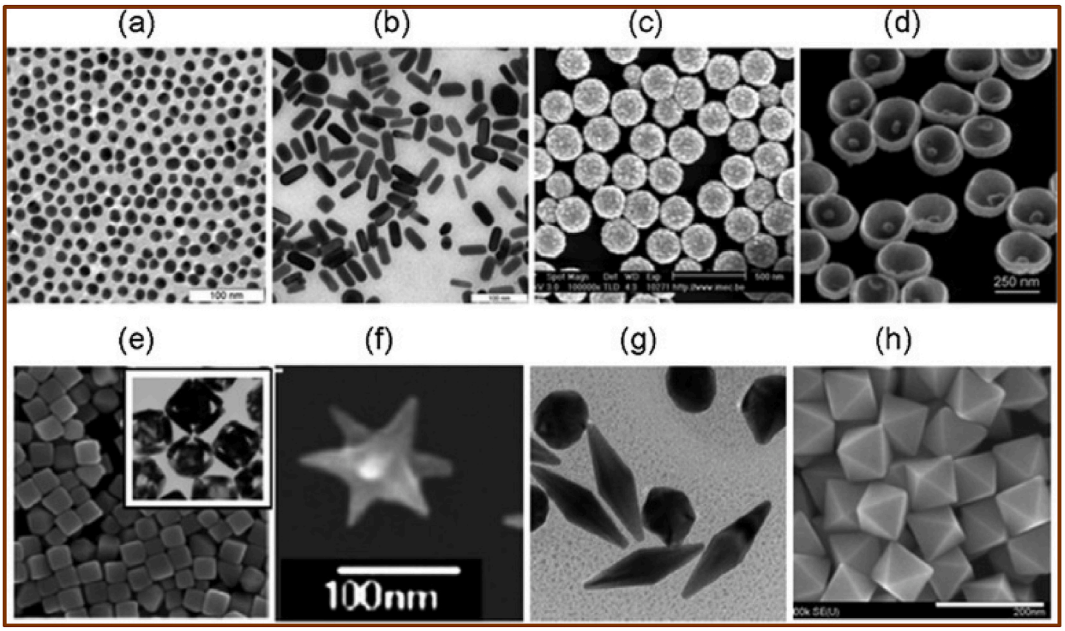

Fig. 11. Different morphologies of gold NPs. Reprinted with permission. Copyright 2018, Springer [49].

thickness on pulse PA signals, with silica-gold core-shell NPs demonstrating superior PA conversion efficacy compared to gold-silica core-shell and gold nanosphere geometries [50]. These findings have facilitated the design of effective nanoprobes for PA tomography, PA imaging, photothermal therapy, and drug delivery.

For molecular imaging purposes, NP-augmented PA techniques have emerged as a dominant approach [51]. This technique involves suspending plasmonic NPs in weakly absorbing fluids to generate PA signals. The PA signal of gold nanospheres, for example, is influenced by heat transfer between the surrounding environment and the NPs, with varying silica shell thickness.

PA imaging techniques have gained significant prominence in the biomedical field. Numerical simulations have been employed to understand the characteristics of PA signals generated by different shapes of NPs. These simulations require complex mathematical formulations, making them computationally expensive. As an alternative, the K-wave simulation toolbox has been implemented to simulate the generated PA signals for various NP shapes, such as cylinders, spheres, hollow cylinders, hollow cubes, cubes, nano stars, and triangles. Ultrasound detectors or point sensors have been used to detect the PA signals, which are presented in both the frequency and time domains to better understand the influence of different shapes on the PA signal characteristics. Detectors placed at multiple locations have been used to observe changes in PA signal characteristics relative to position. Experimental validation has provided valuable insights into the relationship between NP shape and the generated PA signal. The simulation time has been significantly reduced to 40 ns, a substantial improvement compared to other analytical methods that typically require several hours [52].

Gold nano shells have emerged as a new contrast-enhancing agent for PA tomography. These concentric sphere NPs consist of a dielectric silica core and a gold shell. By varying the relative thickness of the shell and core layers, the optical resonance (plasmonic-derived) of gold can be shifted across a wide range of wavelengths, spanning from visible to infrared, where physiological transmissivity is highest. For instance, gold nano shells with a 20-nm gold shell thickness and a 100-nm silica core diameter exhibit an optical absorption peak at 800 nm, enabling the *in-vivo* imaging of the vasculature architecture in the rat brain [53]. The use of gold nano shell contrast agents allows for accurate imaging of the rat brain, with the nano shells significantly enhancing the near-infrared contrast present in the vasculature. This opens up possibilities for biomedical applications, including the detection of tumors in situ and the guidance of tumor therapy based on nanoshells. These findings provide a precise and non-invasive method of imaging at cellular and molecular levels, facilitated by contrast agents.

Gold nanorods and nanospheres have been characterized for their potential in photothermal therapy and PA imaging. Colloids of gold nanorods and nanospheres have been synthesized using seed-mediated methods, and a comparison has been made between finite element simulations and nanosecond PA and photothermal analyses of the NPs. This comparison has helped quantify the size-dependent enhancement of PA signals in nanorods and nanospheres. The non-sphericity of nanospheres has been found to have a greater impact on PA signal enhancement. Nanosecond pulsed PA studies on nanorods have revealed that an aspect ratio of 4.8 generates optimal PA signals. The nanorods, when exposed to nanosecond laser pulses, undergo size and shape variations, which have been confirmed by transmission electron microscopy measurements and optical absorbance. Moreover, simulations involving nanorods of varying diameters and aspect ratios have been conducted to explore photothermal stability and PA signal enhancement. Among the tested nanorods, those with an aspect ratio of 5 and a diameter of 10 nm have been identified as the most suitable for photothermal stability and PA signal generation [54].

In recent times, nanotubes have been widely employed in phototherapy and imaging techniques. Light-triggered treatments for growth inhibition and tumor ablation have been achieved using photothermal therapy and photodynamic therapy [55]. However, a common challenge in these fields is the lack of effective and selective agents that can accumulate in tumors to achieve therapeutic concentrations. Researchers have made attempts to produce photosensitizer complexes with photothermal nanoparticles. For example, a CD44-targeted PA nano-photo therapy agent was developed by conjugating Indocyanine Green (ICG) to hyaluronic acid nanoparticles (HANPs) encapsulated with single-walled carbon nanotubes (SWCNTs). This resulted in a theranostic nanocomplex called ICG-HANP/SWCNTs (IHANPT). The physical properties of IHANPT were fully characterized, along with PA imaging, photodynamic therapy, and photothermal therapy in both in vivo and in vitro settings. The delivery of IHANPT nanoparticles led to their accumulation in tumors in a xenograft human cancer model in nude mice, which was confirmed by PA imaging techniques. The phototherapy effects were verified through low-power laser irradiation, resulting in rapid

temperature increases in the tumor due to the photothermal effect from SWCNTs and ICG. This led to marked tumor induction and significant tumor growth inhibition with IHANPT. The active thermal stability of IHANPTs ensured that photothermal therapy did not interfere with ICG-dependent photodynamic therapy. Thus, the synthesized nanocomplex IHANPT exhibited excellent therapeutic and imaging properties, enabling image-guided photodynamic and photothermal cancer therapy at a cellular and molecular level.

In conclusion, various shapes of nanoparticles, including core-shell structures, nanorods, nanocages, nanospheres, and nanotubes, offer unique advantages and have found applications in biomedical imaging, therapy, and contrast enhancement for photoacoustic techniques. These nanomaterials provide opportunities for precise and non-invasive imaging, as well as targeted therapy at the cellular and molecular levels.

4.2. Effect of size variation

As discussed previously, the structural features of nanoparticles (NPs) have a significant impact on their properties. In addition to different shapes, it is important to analyze the variations in properties resulting from a wide range of sizes. While gold and silver NPs have been widely used for photoacoustic (PA) imaging as molecularly targeted contrast agents due to their advantageous absorption cross-sections [52,57–63], it is worth exploring the performance of NPs made of other materials at different sizes as well.

In the context of gold NPs, for example, the optical properties vary with changes in size, as shown in Fig. 12. The absorption cross-section of spherical gold NPs with a size of 40 nm is approximately five times higher than that of commonly used organic dyes. This

property makes labelling a molecular target with a single alternative of such NPs equivalent to using several other organic dyes [64]. In addition, studies have demonstrated the enhancement of organic dyes and aggregates encapsulated in liposomes or micelles, enabling the delivery of a large number of chromophores for biomolecular imaging. Although still in the early stages of development, this approach holds significant potential for molecular PA imaging [65–68].

While gold NPs with a core diameter greater than 20 nm have been implemented in PA imaging involving specific molecules [69–73] exceeding the renal clearance threshold of 5–10 nm [74–78], their non-biodegradable nature can lead to potential issues such as chronic inflammation and related effects [79,80]. To address these concerns, ultra-small, targeted gold NPs with core diameters less than 10 nm have been developed to improve body clearance, organ biodistribution, and tissue penetration. Hence, the size variation of nanoparticles directly impacts their usage and leads to different properties of the same material.

Further computational investigations have been conducted to analyze the size dependencies of PA effects. A mathematical model based on the Rayleigh-Plesset model has been proposed to explain the trends in PA effects generated by laser-induced nanobubbles in a colloidal gold solution [81]. The model has been validated through measurements and provides accurate approximations for spherical gold NPs in the size range of 10–80 nm. Additionally, it has been demonstrated that metals with tunable plasmon resonance absorptions in the visible and near-infrared regions have additional advantages for PA signal detection. The interaction of lasers with NP suspensions in aqueous media has found applications in medical imaging, biosensors, and therapeutic applications. These NPs absorb laser radiation, resulting in rapid temperature increases and the formation of bubbles in the surrounding medium. These phenomena can enhance the sensitivity of diagnosis based on PA techniques and facilitate better photothermal therapies. Furthermore, semimetal NPs with ultra-small sizes have been utilized in various applications of PA imaging.

In the realm of multifunctional nanoparticles, those with therapeutic and integrated diagnostic functions have gained tremendous attention, particularly in combination therapy for enhanced treatment efficacy. For instance, a multifunctional theranostic agent based on peptide (LyP-1)-labelled ultrasmall semimetal NPs of bismuth (Bi-LyP-1 NPs) was developed [82]. These NPs, synthesized from oleyl-amine as the reducing agent, exhibited greater tumor accumulation after conjugation with the LyP-1 peptide. They showed efficient performance in PA imaging, dual-modal computed tomography, and synergistic NIR-II radiotherapy or photothermal therapy of tumors. Importantly, these NPs could be rapidly cleared through fecal and renal means within 30 days, highlighting their low toxicity and faster clearance as desirable properties for biomedical applications.

It is important to analyze the dependencies of surface plasmon resonance on both shape and size, as they significantly influence material properties. Optical absorption properties of gold NPs with different sizes and shapes are measured using PA methods. Seed-mediated techniques are extensively employed for the synthesis of dot- and rod-shaped gold NPs. Scanning tunnelling microscope measurements are used to determine the size and shape of these NPs [83], enabling the understanding of surface plasmon resonance splitting into transverse and longitudinal modes, particularly in the case of gold nanorods. An increase in the nanorod aspect ratio leads to a redshift in longitudinal surface plasmon resonance. This phenomenon can be utilized to assess variations in the dielectric constant of the surrounding medium with aspect ratios.

Experimental support exists for the simulation of PA signals in gold-silver alloy NPs. Finite element-based numerical analyses have been conducted to compute PA signals for various types of NPs. Monodisperse and size-controlled spherical gold NPs with tunable plasmonic resonance wavelengths have been synthesized using gold-silver alloys. Combining the thermodynamic, electromagnetic, and acoustic properties through a coupling approach, researchers have investigated the impact of the molar fraction of gold NPs in

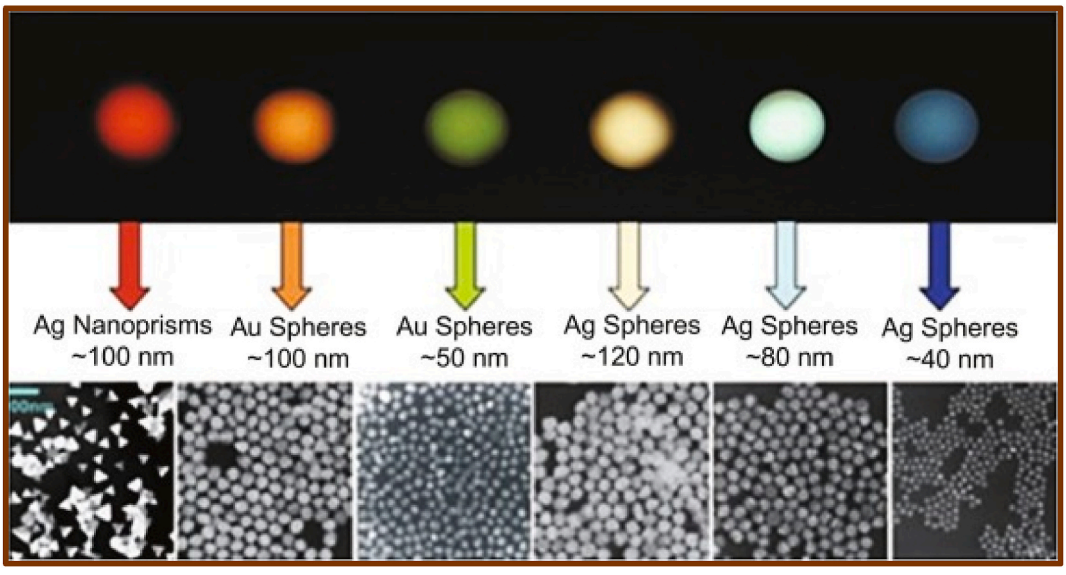

Fig. 12. Variation of optical properties of Au and Ag NPs with varied sizes. Reprinted with permission. Copyright 2019, Optica Publishing Group [56].

gold-silver alloys on the PA signal generation for different NP sizes. Notably, a significantly stronger PA signal was achieved using gold-silver alloys with gold molar fractions of 0.55 and 1, compared to pure silver NPs, while maintaining the same shape and size [84].

While manipulating NP size offers various advantages, there are also limitations and challenges associated with it. As mentioned above, non-biodegradable NPs, such as gold NPs, can lead to chronic inflammation and related effects. To mitigate these issues, researchers are exploring strategies to improve biocompatibility, reduce toxicity, and enhance clearance mechanisms. Additionally, the design and synthesis of NPs with optimal sizes for specific applications require careful consideration of factors such as biodistribution, clearance pathways, and potential long-term effects on the body.

4.3. Role of composition, alloys and hybrid materials

The previous section illustrated the influence of size and shape on PA imaging, a commonly used biomedical imaging and detection technique. PA techniques offer advantages such as non-invasiveness, low cost, and non-ionizing characteristics, which make them valuable in high yield results. This has led to further investigation into developing contrast agents with varying compositions and hybrid properties.

To enhance the contrast for in vivo imaging ("Fig. 13"), gold NPs have been commonly employed as potential sonophores due to their good absorption cross-section and highly tunable plasmonic resonance [86]. However, their utilization in clinical applications is hindered by low PA efficiency and toxicity. Therefore, there is a high demand for the development of colloidal PA agents that can work within the tissue transparency window, provide good PA signal, and exhibit biocompatibility. Previous findings demonstrated the coating of gold NPs of various shapes and sizes with melanin shells, resulting in hybrid NPs with better biocompatibility, excellent dispersibility, and enhanced PA responses compared to pure gold or pristine melanin particles [87]. Among different geometries, the rod-shaped NPs showed better performance, which was further validated through numerical calculations explaining the improved performance due to a thermal confinement effect. The melanin-coated gold NPs were utilized as gastrointestinal imaging probes in mice (see Fig. 14).

This imaging method signifies the non-ionizing modality and the improvement in performance achieved by employing a hybrid model that provides adequate spatial resolution and good tissue contrast [88–104]. Emphasis was also placed on molecular and functional imaging achievable through in vivo PA imaging. In this regard, recent advancements in colloidal gold nano beacons for molecular PA imaging were reviewed [105]. These nano beacons represent a stringent NP platform that can emulate several copies of minute gold NPs (ranging from 2 to 4 nm) within a larger colloidal particle, which is encapsulated by natural amphilines or biocompatible synthetics. The use of multiple tiny gold NPs amplifies the PA signal without exceeding the renal elimination threshold size. Fibrin-targeted gold nano beacons have shown promising results in the detection of microthrombus during ruptured atherosclerotic plaques, allowing the identification of patients at risk of lumen stenosis and stroke. Smaller gold nano beacons have facilitated the advancement of sentinel lymph node biopsy and assessment, providing improved rapidity and sensitivity in mice. Moreover, in vivo application has shown the advantages of specific discrimination, sensitivity, quantification, and integrated visualization of angiogenesis, a vital microanatomical biomarker of cardiovascular disease progression and tumors.

In the field of photothermal therapy, a major challenge is to develop biocompatible transducers with the capability to efficiently absorb and convert near-infrared light into heat energy [106]. A study reported the salt-induced aggregation of gold NPs for PA imaging and photothermal therapy of cancer [107]. These NPs, when dispersed in a biocompatible medium, can form efficient transducers for photothermal or PA imaging for cancer diagnosis. The in-situ aggregation of gold NPs induced by salt leads to good near-infrared absorption through plasmonic coupling between nearby gold NPs. The recorded photothermal conversion efficiency was 52 %, resulting in the photothermal destruction of tumor cells. Notably, the simultaneous PA imaging and photothermal therapy of tumors using in-situ aggregates of gold NPs provide an effective and simple way to develop new biocompatible and intelligent photothermal transducers with improved PA imaging and photothermal efficiency.

Similarly, another study reported the synthesis of silver NPs in ethanol using the laser ablation method, where the pulsed PA technique was used [108]. Pure metal NPs, particularly silver NPs, have gained attention due to their unusual properties related to

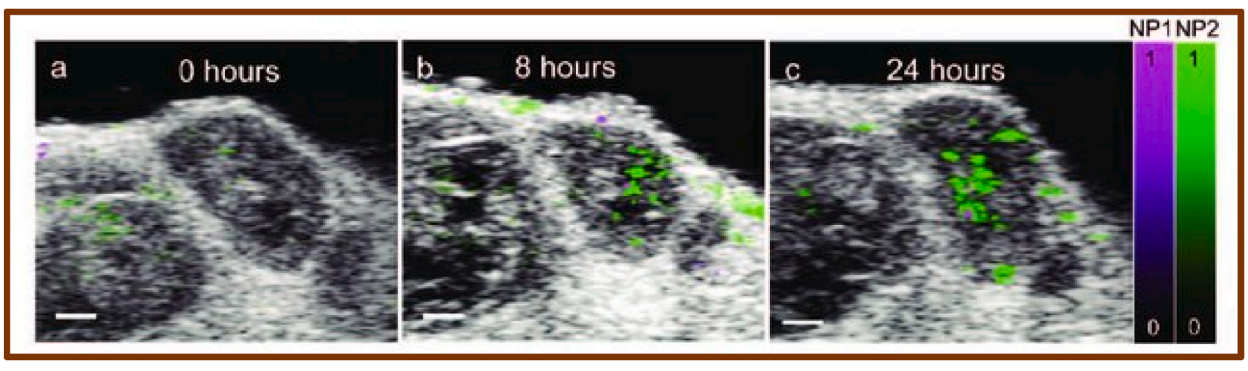

Fig. 13. Accumulation of contrast agent within a targeted tumor using two different NPs. Reprinted with permission. Copyright 2015, ACS Publications [85].

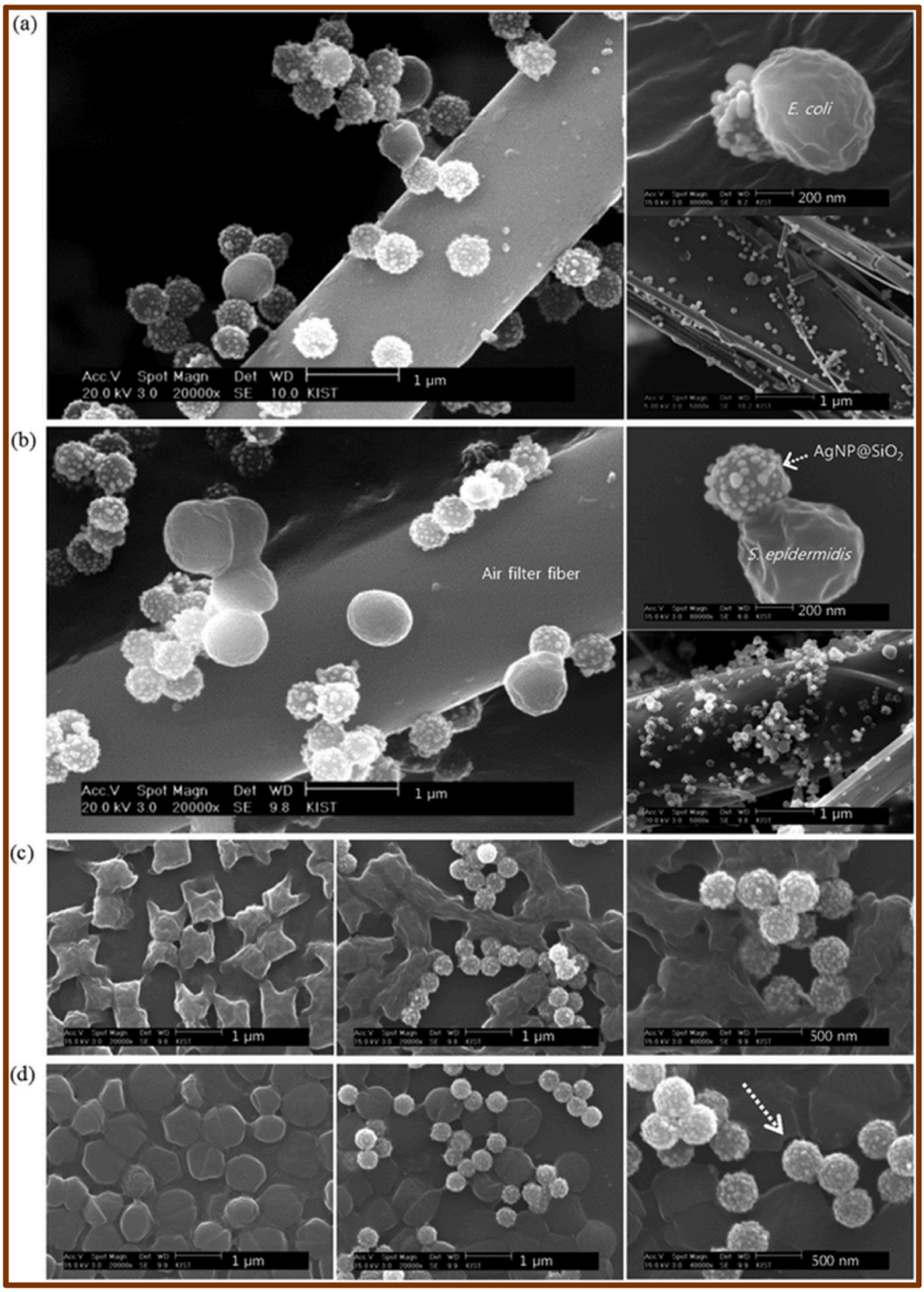

Fig. 14. Scanning electron microscope images of (a) *E. coli* and (b) *S. epidermidis* deposited on the AgNP@SiO2-coated air filter at different magnifications and (c) *E. coli* and (d) *S. epidermidis* incubated in AgNP@SiO2 solution for 0, 10, and 30 min (left, middle, and right, respectively). Reprinted with permission. Copyright 2012, ACS Publications [113].

electrical, optical, and magnetic properties [109,110]. The PA technique was employed to analyze the rate of production per laser pulse and the concentration of the synthesized silver NPs. The samples were produced using a Nd:YAG laser with a pulse duration of 7 ns and a wavelength of 1064 nm. The laser pulse energy ranged from 10 to 100 mJ, and transmission electron microscopy confirmed

that the attained NPs had a spherical geometry with an average size of approximately 10 nm. The plasmon absorption peak was observed at 400 nm through the absorption spectra of the colloids. Furthermore, a significant decline in the production rate of silver NPs was observed during the initial hundreds of laser pulses, after which the production rate became almost constant. This study concluded that the laser pulse fluence on the surface of the target was directly proportional to the root mean square value of the generated PA signal, highlighting the pivotal use of the PA technique in monitoring the ablation process.

In order to make PA applications a powerful biomolecular imaging technique in vivo, it is crucial to develop efficient and safe contrast agents. Despite their low invasiveness, high spatial resolution, and greater penetration power, PA techniques still face challenges in developing endogenous, non-toxic, photostable, and biocompatible contrast agents, especially for clinical purposes [111]. Studies have been conducted to address the aforementioned issues, particularly poor aggregation and high PA contrast [112]. MelaSil_Ag-NPs, a biocompatible PA nanoprobe, was developed, relying on the formation of silica-templated eumelanin and metal chelating properties. This nanoprobe can reduce unipositive silver ions and control the growth of the generated metal NPs. The self-structuring system in a core-shell architecture of the hybrid nanoplatforms enables the silver core to boost the PA signal, despite the low eumelanin content. These nanoplatforms exhibit stable PA properties even under greater irradiation. Furthermore, the conjugation with rhodamine isothiocyanate enables particle detection through fluorescent imaging, showcasing their multifunctional characteristics. The nanoplatforms are stable against aggregation and can be adequately endocytosed by human pancreatic cells without cytotoxic effects. These features make them promising multifunctional platforms for bio-medical applications.

The advantages of both gold and silver NPs have led to the combination of their properties. Silver ions have excellent antibacterial properties [114], and silver NPs act as reservoirs for these ions. This enables targeted therapy for bacterial infections. Previous investigations have focused less on understanding the effective release and monitoring of these ions from silver NPs. However, a study was conducted to develop hybrid NPs by coating gold nanorods with silver. This coating decreased the PA signal. The resulting nanorods were stable under normal conditions, but when exposed to a 1 mM ferricyanide solution, the silver shell underwent oxidative etching. The PA contrast simultaneously recovered as the silver was released, providing better non-invasive monitoring of the released silver ions. The released silver ions exhibited strong antibacterial efficacy comparable to that of free silver ions (AgNO3). The NPs effectively killed over 99.99 % of both gram-positive and gram-negative Escherichia Coli. Additionally, a pilot in-vivo experiments demonstrated the theranostics capacity of the gold-silver nanorods by inoculating mice with methicillin-resistant *Staphylococcus aureus* subcutaneously implanted after silver etching. The results showed a 730 % increase in the PA signal before and after etching, along with a 1000-fold reduction in bacterial counts in the infected tissues compared to the untreated control [115]. Moreover, these hybrid NPs can release silver ions upon stimulation by reactive oxygen species such as peroxynitrite and hydrogen peroxide. Thus, these NPs hold great potential as theranostics agents for PA imaging and the treatment of bacterial infections.

In recent studies, attention has shifted towards NPs coated with bioactive materials (Fig. 15) for biomedical applications. One investigation focused on iron oxide NPs coated with boiling rice starch extract for PA imaging-guided chemo-photothermal therapy to treat cancer [116]. The synthesis of iron oxide NPs involved a solvothermal method. The rice starch-loaded doxorubicin (DOX) molecules were physically immobilized on the surface of the iron oxide NPs. In vitro drug release was assessed in acidic (pH 4.5), neutral (pH 7.2), and basic (pH 9.0) media over varying time periods using UV spectroscopy. The physical and chemical properties of these spherical NPs were characterized using advanced instrumentation. The potential for hyperthermia was evaluated through a magnetic saturation experiment with rice starch iron oxide NPs in targeted drug delivery. The biological activity was analyzed using the acridine orange/propidium iodide fluorescence cell viability study and the 3-(4,5-dimethylthiazol-2-yl)-2,5-diphenyl tetrazolium bromide assay. The synthesized NPs demonstrated good photothermal stability, excellent photothermal conversion efficiency, high absorption in the infrared region, and biocompatibility. These findings support further analysis of rice starch as an excellent bioactive coating material for theranostics applications (see Fig. 16).

Melanin, a natural pigment, can serve as a biomarker for melanoma [117]. Studies have described its utilization as a contrast agent [118]. Furthermore, gadolinium-loaded synthetic melanin NPs exhibited significantly higher PA signal intensity. Specifically, they demonstrated a 40-fold enhancement in PA signal intensity compared to synthetic melanin and other metal-chelated synthetic melanin

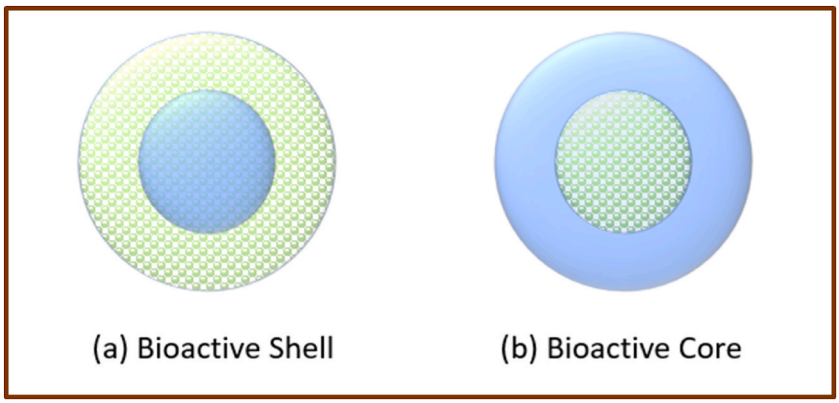

Fig. 15. Illustration of different bioactive models.

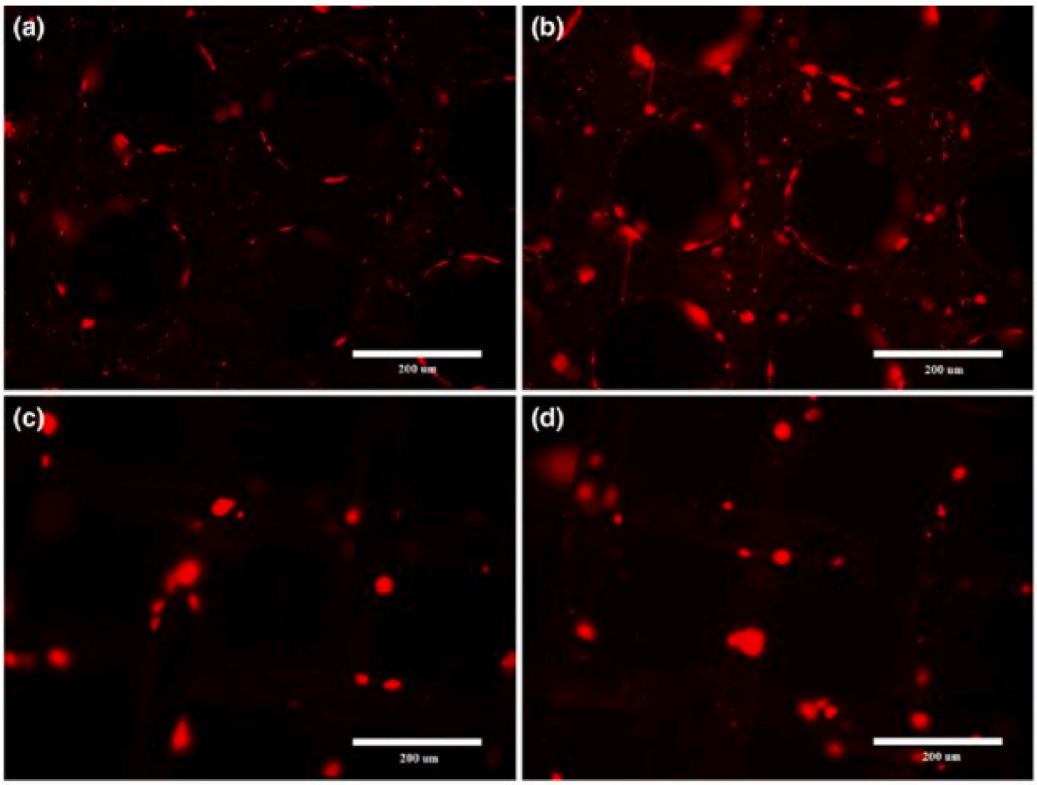

Fig. 16. Human leukaemia monocytic cell lines are attached to the mesh as a consequence of the cell tracker experiment. Cell tracker dye solution was used to colour the cells red. (a) without and (b) with dodeca molybdophosphoric acid; stainless steel mesh (c) without and (d) with dodeca molybdophosphoric acid. Reprinted with permission. Copyright 2014, RSC [135].

NPs [119]. This makes them suitable as dual-labeling agents, as they also serve as effective contrast agents in magnetic resonance imaging. These NPs were employed to label human mesenchymal stem cells, and cellular uptake was confirmed using bright-field optical and transmission electron microscopy. The stem cells labelled with gadolinium-synthesized NPs expressed the surface markers CD90, CD73, and CD105. The labelled stem cells were injected intramyocardially into mice, and the tissue was observed using PA and magnetic resonance imaging. The results indicated an increase in cell number accompanied by the PA signal, demonstrating that this approach could be used to differentiate between stem cell populations with a limit of detection of 2.3 × 104 cells. The combination of multimodal magnetic resonance and PA imaging offers a temporal solution for PA imaging along with the anatomical resolution of magnetic resonance.

Similarly, copper sulfide NPs have emerged as a new class of PA contrast agents for imaging deep tissues [120]. Previous findings have shown that copper sulfide NPs exhibit quantum size confinement and can generate heat for photothermal ablation of cancer cells when interacting with 800-nm light [121,122]. Semiconductor copper sulfide NPs were utilized for PA tomography using an Nd: YAG laser at a wavelength of 1064 nm [123]. These NPs were employed to visualize the brain of a mouse after intracranial injection. Additionally, the NPs were tested with agarose gel in chicken breast muscle at a depth of 5 cm.

Similarly, nickel (II) dithiolene-containing polymeric NPs have been utilized for deep tissue imaging in the second near-infrared window [124]. These nascently developed polymeric NPs exhibit a sharp and strong absorption peak at 1064 nm, making them suitable as contrast agents for enhancing specific absorbance in the near-infrared window, particularly for deep tissue imaging in vivo. In vivo PA images of deep tissue, such as lymph nodes (sentinel), bladders, and gastrointestinal tracts in live rats, were acquired using a clinically viable imaging system. The PA signal enhancement achieved by these synthesized NPs in the near-infrared II window (wavelength range ~1000–1700 nm) was 287 % higher than that in the near-infrared I window (wavelength range ~700–900 nm). These results demonstrate the strong absorption capability of these NPs in the near-infrared II window and indicate the feasibility of PA imaging for clinical and preclinical investigations, as shown in in vivo and ex vivo PA imaging of gastrointestinal tracts and bladders in rats. These findings can be translated to human clinical evaluation [125,126].

Similarly, multifunctional nanoparticles (NMs) with both therapeutic and diagnostic functions and low toxicity have gained significant attention [127,128]. To this end, research was conducted on PEGylated W-doped TiO2 (WTO) NPs synthesized via a facile organic route [129]. The study demonstrated the strong absorbance of these WTO NPs in the second near-infrared window, resulting from successful doping with tungsten (W). These NPs can absorb both ionizing radiation and NIR-II laser, making them suitable for dual-mode tomography NIR-II PA imaging. Long-term in vivo studies confirmed that the PEGylated WTO NPs were non-toxic and could

be cleared from the specimen after 30 days, opening up potential applications in therapeutics and imaging in biomedicine.

With a broad overview of applications involving pure metals and hybrid materials as contrast agents, nanotechnology has made significant progress in non-invasive molecular imaging techniques, surpassing the limitations of conventional optical imaging techniques in terms of imaging depth. This progress has created new opportunities in clinical applications, translational medicine, and fundamental biology. Recent advancements in the field include the use of organic NPs for PA imaging applications. Organic NPs have been categorized based on their diverse imaging applications, including gastrointestinal imaging, tumor imaging, disease microenvironment imaging, sentinel lymph node imaging, and real-time drug imaging [130].

Similarly, to advance the clinical and preclinical applications of PA imaging, novel PA contrast agents are highly sought after for molecular imaging of diseases, particularly to overcome the limitations in depth and resolution [131]. Perylene-3,4,9,10-tetracarboxylic diimide-based near-infrared-absorptive organic NPs have been formulated as effective agents for PA imaging of brain tumors in live mice, offering improved permeability and retention [132].

In addition to metallic and organic NPs, assembled NPs from various organic molecules have shown versatility for theranostic applications. Studies have been conducted on chlorin dimers synthesized by reducing porphyrin molecules [133]. These dimers assemble into aggregates in the absence of auxiliary agents or surfactants [134]. The resulting NPs exhibit higher absorbance than their porphyrin counterparts, leading to enhanced photothermal and photodynamic activity. These NPs have been effectively endocytosed by tumor cells under irradiation, resulting in suppressed tumor growth in vivo. Moreover, these aggregates can be utilized for PA imaging and, when combined with phototherapeutic capabilities into a single NP, can contribute to diagnosis, imaging, and therapy in the future.

The fundamental unit of both dimers and polymers is a minute monomer. Polymer encapsulated NPs have gained prominence in the field of biomedicine due to their ease of fabrication, unique optical properties, and better performance in therapeutic and imaging agents [132–134]. Fluorogenic or conjugated polymers with aggregation-induced emission feature significant advantages in tuning brightness, biocompatibility, physical stability, and potential biodegradability. To enhance readability, the latest development in polymer-encapsulated conjugated polymers is summarized, including preparation methods, matrix selection, material design, surface functionalization, and NP fabrication.

Similarly, the specific applications regarding a target in vivo and in vitro, such as cell labelling, cell tracing, blood vessel imaging, molecular imaging, and inflammation monitoring, are focused upon. The strategies to fine-tune the NP properties by altering the organic cores and selecting polymer matrices are discussed [136]. However, it is important to provide sufficient context for the studies or findings discussed. For example, the passage does not explain why a particular type of NP is important or how its properties contribute to its applications. This lack of context makes it difficult to understand the significance of the findings.

Likewise, in the case of PA vascular imaging, conjugated polymer NPs have been widely used. Exogenous contrast agents with perfect near-infrared absorption are favorable for satisfactory penetration depths. Poly[9,9-bis(4-(2-Ethylhexyl)phenyl)fluorene-alt-co-6,7-bis(4-(hexyloxy)phenyl)-4,9-di(thiophene-2-yl)-thiadiazoloquinoxaline] (PFTTQ), a conjugated polymer, was synthesized using Suzuki polymerization [137]. PFTTQ NPs exhibit high non-radiative quantum yield and strong near-infrared absorption, making them suitable for photothermal therapy [138–141]. Additionally, these NPs demonstrate better photostability than gold nanorods under high pulsed laser illumination at a fixed laser fluence of 15 mJ cm^{-2}. The significance of PFTTQ NPs as a good PA probe is demonstrated using brain vascular imaging as an example.

Polymeric NPs, particularly natural polymers like cellulose NPs, have gained attention due to their biodegradability and potential use as PA contrast agents [142]. The following NPs were analyzed, and the outcomes illustrated a peak PA signal at 700 nm and an in vitro detection limit of 6 pM. Mouse models of ovarian cancer were used for PA imaging. PA imaging is widely used in many preclinical models related to human disease, including breast [8], prostate [143], and ovarian cancer [144]. Notably, these NPs were found to be biodegradable in the presence of cellulose, as observed through electron microscopy and glucose assay.

With the increase in opportunities for formulating different types of NPs, the field of PA imaging has gained new momentum by utilizing semiconductor NPs. Semiconductor polymer NPs with a self-quenched process were developed by incorporating an electron-deficient unit into the backbone of semiconducting polymers [145]. These NPs were transformed into semiconducting polymer NPs, which amplified PA imaging in live mice by 1.7-fold compared to semiconductor polymer NPs. Furthermore, the delineation of tumors was enhanced by 4.7-fold after systemic administration.

Semiconductor polymer NPs were tested for second near-infrared PA imaging. They proved to be useful for deep-tissue diagnosis due to minimized tissue absorption and reduced light scattering [146]. These organic nano agents consist of a pi-conjugated and oxidizable polymer as a PA signal generator and a hydrolysable polymer as a particle matrix to enhance water solubility. Moreover, these NPs can be cleared via renal excretions and hepatobiliary pathways after systemic administration, thus minimizing potential toxicity to living mice. The nano agents exhibit excellent photothermal conversion efficiency and emit signals at 1064 nm, providing sensitive near-infrared-II PA imaging of deep brain vasculature and subcutaneous tumors at a low systemic dosage. The findings discussed provide valuable insights into semiconductor materials for biophotonic applications, mainly in the near-infrared-II window.

Another study focused on the synthesis of a broadband-absorbing PA contrast agent based on semiconductor polymer NPs [147]. This contrast agent was applied for PA imaging in the near-infrared-II window and can absorb in both I and II regions, allowing for a comparison of PA imaging at 750 nm and 1064 nm. The synthesized NPs resulted in a 1.4-fold greater signal-to-noise ratio for PA images at 1064 nm compared to 750 nm at an imaging depth of 3 cm. The study demonstrated imaging of brain vasculature in living mice, which exhibited a 1.5-fold higher signal-to-noise ratio compared to near-infrared-I imaging of PA signal. The work highlights the advantages of near-infrared-II over near-infrared-I for PA imaging and introduces a broadband-absorbing contrast agent for improved PA imaging.

Alongside an eclectic range of nanomaterials, the implementation of green techniques in synthesizing NPs is a trending research

field in nanotechnology. A one-spot green technique was demonstrated, which elaborated on the rapid surface passivation of carbon NPs with organic molecules such as polyethylene glycol and polysorbate in a solvent-free condition [148]. These NPs, derived from commercial food-grade honey, have a size of approximately 7 nm, different from previously explored NPs like carbon nanotubes, copper NPs, and other gold NPs. The results of the study illustrated an exceptional signal enhancement of sentinel lymph nodes, potentially reducing complications caused by low-resolution imaging or dye mismarking.

Simultaneously, studies have been conducted on the optothermal properties of inorganic NPs for PA applications [149]. Plasmonic systems were found to be more favorable than dye molecules for generating PA signals for imaging and spectroscopy due to their enhanced versatility. The properties of inorganic NPs can be adjusted to achieve the desired plasmonic properties, allowing for analysis across a wide range of the spectrum. Surface chemical modifications enable the introduction of desired functionalities. The conversion efficiency, which represents the efficacy of transforming light into heat in PA signals, can be precisely determined using various PA methods.

Solventless preparation of PEGylated black phosphorus NPs was carried out for photothermal therapy and PA imaging of cancer [150]. Black phosphorus and other nanostructures have gained considerable attention due to their unique properties and broad range of use cases in biological, physical, and chemical fields. Biocompatible PEGylated black phosphorus NPs were prepared, and their properties, such as conversion efficiency and photostability, were demonstrated, making them suitable as PA imaging and photo-theranostic agents for cancer. They showed good accumulation capacity at the tumor location and achieved photothermal ablation through near-infrared light irradiation.

In addition, alkaline phosphatase-triggered self-assembly NPs were observed to enhance optoacoustic (OA) imaging of tumors [151]. An alkaline phosphatase activatable probe was reported for improved PA imaging, along with the NIR probe IR775-Phe-Phe-Tyr (H2PO3)-OH (1P), which was used for in vitro alkaline phosphatase activatable PA imaging. The catalysis of alkaline phosphatase resulted in the conversion of 1P to IR775-Phe-Phe-Tyr-OH, which self-assembled into NPs. The formation of self-assembled NPs led to a 6.4-fold enhancement of the 795 nm PA signal of 1P. The future scope of all the discussed NPs and their implementations will be further explored in the subsequent section.

5. Future scope & conclusion

Over the past two decades, various types of NPs have found widespread use in commercial development, offering opportunities for breakthroughs in nanotechnology by leveraging size, shape, composition, and hybrid material properties (Fig. 17) [152–156]. Applications include products like stain-repellant fabrics, crack-resistant paints, and self-cleaning windows, harnessing nanoscale features for cleaner, lighter, and stronger systems. For instance, transparent nanoscale titanium oxide NPs are used in sunscreens, while

Fig. 17. Future scope of NPs.

antimony-tin oxide NPs enhance scratch resistance and UV protection in coatings. Nanotechnology has also improved safety in the automotive industry with NPs enhancing tire grip and reinforcing steel [153]. In food manufacturing, NPs can manipulate molecular food forms and improve packaging with antimicrobial coatings [156]. In medicine and biology, NPs are utilized in drug delivery [157], gene therapy [158], imaging [159], and many other applications [159–166]. In view of these ongoing developments, NPs hold promise in therapeutic applications, especially in cancer diagnosis and treatment, while research must address potential toxicity concerns [167–169] damage to the cardiovascular and respiratory systems [170,171], and inflammatory responses [172].

These above-mentioned avenues create new opportunities for future research and potential developments of novel bio-applications and advanced technologies. Likewise, despite the stupendous capabilities that were demonstrated by these miniature materials, emphasis should also be placed on the imaging and instrumentation systems for better analysis and validated results. Light sources for better PA signal excitation are one of the aspects with tremendous potential in the work related to light sources. The advantage of PA in enabling valuable insights into investigating turbid mediums in comparison with other methods made the technique revolutionize the applications of bio-optical observation systems.

In the realm of pre-clinical applications, a multitude of both established commercial and experimental imaging scanners, already in operation within research laboratories globally, have been pivotal in addressing key research challenges. These encompass a wide spectrum of biological functions, ranging from investigations into cardiovascular diseases [173], cancer cells [174], and tumor therapy [175], to applications in ophthalmology [176], neuroimaging [177], diabetes [178], obesity [179], cell trafficking [180], and immunology [181].

Also, the growing integration of nanotechnology and chemistry into this field opens up a vast array of applications and holds considerable potential for synthesizing various NPs. This progress offers a promising solution to impending challenges across various domains, including the creation of targeting agents, organic dyes, and specialized biomarkers. Harnessing the capabilities of nanotechnology and chemistry, researchers can effectively confront these challenges, investigating innovative solutions across diverse areas like diagnostics, therapeutics, biomedical research and biomedical imaging.

Through the synthesis of NPs using these scientific disciplines, precision targeting, advanced imaging capabilities, and improved molecule detection can be achieved, ultimately propelling precision medicine and diagnostics forward. This interdisciplinary approach is expected to revolutionize disease diagnosis and treatment, opening up new avenues for personalized medicine and targeted therapies. In accordance with enhancing contrast agents, there is a need for the development of cost-effective and efficient technologies that offer increased sensitivity, miniaturization, ultrasound detection methods, expanded data processing capacities, and integrated inversion models. These implementations will continue to drive the evolution of PA technology, positioning it at the forefront of research, and improving the tools necessary for clinical diagnostics and biological research studies.

At present, multiple solid-state lasers have been employed in clinical applications for stent and vascular imaging, typically operating at a single wavelength. Consequently, there is a pressing demand for novel light sources characterized by high-output pulse energy and rapid wavelength tuning to facilitate improved clinical translation in the realm of PA imaging.

Continuing in this field, recent advancements have introduced light-emitting diodes and laser diodes as promising alternatives to conventional solid-state lasers [182]. These diodes offer distinct advantages, such as smaller sizes, cost-effectiveness, and a broader spectrum of wavelengths compared to their solid-state counterparts. These attributes make them particularly well-suited for real-time PA imaging applications in clinical diagnostics. However, it's essential to address certain challenges that persist, such as low signal-to-noise ratios and inadequate output energies.

To tackle these challenges, researchers are exploring techniques like pulsed light with coded excitation and the averaging of multiple signal acquisitions [183]. These approaches hold the potential to enhance the performance of diode-based PA imaging systems, further advancing their utility in clinical diagnosis and research.

The ongoing development of these innovative light sources holds immense promise for advancing imaging applications in areas concerning vasculatures, tumors, invasive devices, red blood cells, and atherosclerotic plaques. Moreover, laser diodes can be designed and miniaturized into curved arrays, offering potential advantages for probe design. Notably, these laser diodes show great potential in the creation of miniature PA imaging systems, characterized by their compactness and cost-effectiveness. As a result, they are poised to become the future light sources of choice for clinical and real-time PA imaging systems, representing a significant step forward in medical imaging technology.

Furthermore, the integration of ultrasound sensors holds great significance when combined with laser diodes [184] and PA imaging techniques [185,186], offering a broad spectrum of applications. Ultrasound sensors offer distinct advantages over conventional piezoelectric counterparts, including immunity to electromagnetic interference, transparency, heightened sensitivity, and broadband capabilities. These attributes enhance their compatibility with intraoperative Magnetic Resonance Imaging (MRI) for guiding surgical procedures. Moreover, ultrasound sensors can be strategically positioned along the path of light, facilitating co-linear design for both ultrasound detection and light delivery. Leveraging these benefits, it becomes possible to miniaturize and integrate probes, maximizing the signal-to-noise ratio without compromising bandwidth and acoustic sensitivity – a prospect with considerable potential for the future.

Conversely, as the active surface area increases, the sensitivity of piezoelectric ultrasound sensors gradually diminishes, presenting a challenge to achieving a good signal-to-noise ratio in images, particularly with miniature detectors. In applications requiring wide bandwidth, detectors made of polyvinyl difluoride [187] become more significant. Although these detectors offer high bandwidth, their sensitivity is generally lower compared to piezo composites due to smaller electromechanical coupling coefficients. However, they do provide a narrower detection bandwidth, particularly with high-frequency detectors, potentially impacting the quality and spatial resolution of collected images.

Therefore, optical ultrasound sensors hold the promise of significantly advancing the development of miniature probes for PA

applications. Various other optical and ultrasound imaging techniques have been explored in the past [188–190] and the integration of these techniques can provide comprehensive structural information about tissues in numerous applications. In some cases, ultrasound was generated using optically absorbing materials coated on a fiber tip through pulsed light illumination via the PA effect [191], further expanding the potential of optical ultrasound sensors in medical imaging.

To further enhance existing implementations and methodologies, pulse-echo signals generated from tissue can be captured by ultrasound detectors for imaging purposes. As part of ongoing advancements, researchers are exploring the use of dye-based, gold, and other NP composites for the development of all-optical dual-mode PA probes. These probes exploit precise optical absorption bands, facilitating the transmission of light for efficient PA imaging.

In addition to intraoperative imaging techniques, point-based PA spectroscopy holds the potential for advancing minimal or non-invasive approaches. It can aid in target identification and the preservation of vital tissue structures, such as blood vessels during tumor resections or nerves during nerve blocks.

While PA imaging is still in its early stages of development, it offers depth-resolved spectroscopic contrast at greater depths compared to traditional optical spectroscopy methods. Consequently, PA imaging has experienced exponential growth, becoming a prominent area of research, especially in biomedical imaging applications. With the potential for transformative impact in clinical and pre-clinical settings, the integration of PA imaging into clinical and diagnostic practices has garnered significant interest and holds considerable significance across various fields. The miniaturization of imaging techniques has the potential to revolutionize PA imaging of deep tissue structures through internal illumination of light, greatly expanding its clinical capabilities.

Given these recent developments, further research is imperative, focusing on sources, detectors, materials, and applications to utilize the full potential of PA in biomedical imaging. PA imaging presents a powerful biomedical imaging modality with several unique advantages. It combines the high resolution of optical imaging with the deeper tissue penetration of ultrasound, enabling visualization of anatomical structures, physiological processes, and molecular signatures within living organisms. However, translating the promise of PA imaging into routine clinical applications requires overcoming certain challenges associated with nanoparticle contrast agents.

A critical challenge lies in ensuring the biocompatibility of PA nanoparticles. Ideally, these agents should be non-toxic, readily cleared from the body after use, and avoid triggering unwanted immune responses. Manohar et al. explored strategies for surface modification of gold nanorods to enhance biocompatibility and reduce aggregation within the body [192]. Liang et al. demonstrated the use of antibody-conjugated carbon nanotubes for targeted PA imaging of tumors, highlighting the potential of targeted approaches [193]. The efficacy of PA nanostructures and nanomaterials primarily relies on their ability to efficiently convert absorbed light energy into acoustic waves. This necessitates careful selection of materials with strong light absorption at wavelengths that can penetrate deep into tissues. Traditional NIR absorbing agents, like gold nanorods, offer good penetration but mostly suffer from limited absorption efficiency. Recently, research by Zha et al. explored novel organic photoacoustic contrast agents with tailored NIR absorption properties for deeper tissue imaging [194]. Developing a broader library of PA nanoparticles with optimized light absorption characteristics remains an active area of research. While PA imaging boasts superior resolution compared to traditional ultrasound, achieving high spatial resolution with deep tissue penetration remains a critical challenge. Factors like limited bandwidth of ultrasound detectors and the scattering of acoustic waves by tissues can compromise image quality.

Research by Zhang et al. investigated photoacoustic microscopy techniques that utilize focused laser beams and high-frequency ultrasound detectors to achieve micrometer-scale resolution for pre-clinical studies [195]. Further advancements in both nanoparticle design and imaging instrumentation are necessary for achieving optimal resolution and image specificity in deep tissues. The integration of PA imaging with other modalities, like magnetic resonance imaging (MRI) or computed tomography (CT), offers the potential for comprehensive characterization of tissues. However, developing PA nanoparticles that are compatible with other imaging modalities presents a significant challenge. Yang et al. explored the development of multifunctional PA/MRI contrast agents for tumor imaging, demonstrating the potential of theranostics (therapy and diagnostics) using PA nanoparticles [196]. Further research is required to create a wider range of theranostics PA nanoparticles for simultaneous imaging and therapeutic interventions. High cost of developing and manufacturing PA nanoparticles can hinder their clinical translation. Additionally, regulatory hurdles and the need for extensive pre-clinical and clinical trials pose significant challenges for bringing PA nanoparticle technologies to the bedside.

Despite these challenges, PA imaging using functional nanostructures holds immense potential for revolutionizing biomedical imaging. The high sensitivity of PA imaging with targeted nanoparticles allows for the detection of diseases like cancer at earlier stages when they are more treatable. Research by Chen et al. demonstrated the use of PA imaging with gold nanorods for the early detection of lymph node metastases, highlighting the potential for improved patient outcomes [197]. PA nanoparticles can be used to guide minimally invasive therapeutic interventions like photothermal therapy or drug delivery. The real-time visualization capabilities of PA imaging enable precise targeting of diseased tissues while minimizing damage to healthy surrounding structures. A study by Zhong et al. explored the use of PA imaging to guide laser ablation of tumors using gold nanorods, demonstrating the potential for image-guided therapies [198]. PA imaging excels at visualizing blood vessels due to the strong light absorption properties of hemoglobin. This opens doors for studying blood flow dynamics, monitoring angiogenesis (new blood vessel formation), and diagnosis of vascular diseases. Research by Zare et al. investigated the use of PA imaging for quantifying blood flow in tumors, highlighting its potential for monitoring treatment efficacy [199]. PA imaging can be used to assess various physiological processes within tissues, such as oxygenation, metabolic activity, and drug delivery. By employing PA nanoparticles sensitive to specific biomarkers, researchers can gain valuable insights into the functional state of tissues.

A study by Xie et al. [200] explored the use of PA imaging with carbon nanotube-based probes for monitoring tumor hypoxia (low oxygen levels), which is a critical factor in cancer progression. The development of PA nanoparticles with unique spectral signatures allows for multiplexing, where several different nanoparticles can be used simultaneously to image various biomarkers within the

same tissue. This can provide a more comprehensive picture of the biological processes at play. Research by Cheheltani et al. demonstrated the use of multicolor PA imaging with different gold nanoparticle morphologies to differentiate tumor types [201]. Further advancements in nanoparticle design and signal processing techniques are crucial for realizing the full potential of PA imaging multiplexing.

In accordance to the above discussion, some other emerging strategies in utilization of PA in biomedical imaging encompass Biodegradable NPs. Developing biodegradable PA nanoparticles that are naturally cleared from the body after use can address concerns about long-term biocompatibility and potential toxicity. Yoo et al. explored the use of poly (lactic-co-glycolic acid) (PLGA) nanoparticles for PA imaging, demonstrating their biodegradability and potential for clinical applications [202]. Engineering PA nanoparticles that respond to specific stimuli, such as changes in pH or enzymatic activity within the target tissue, can enhance image specificity and reduce background noise. Another study by Miao et al. investigated activatable PA probes for tumor imaging that become fluorescent only in the acidic environment of tumors [203]. This approach holds promise for improved diagnostic accuracy. The integration of Artificial Intelligence algorithms into PA image analysis can significantly improve image reconstruction, reduce artifacts, and automate image interpretation. Deng et al. demonstrated the use of deep learning techniques for quantitative PA imaging, highlighting the potential of AI for improved image analysis and data extraction [204]. PA imaging can be used to visualize blood flow dynamics by capturing the motion of red blood cells within blood vessels. This emerging technique, known as photoacoustic flow imaging, has the potential to assess vascular health and diagnose various cardiovascular diseases. Van den Berg et al. explored the use of PA flow imaging for quantifying blood flow in brain tumors, demonstrating its potential for studying tumor angiogenesis [205].

PA imaging NPs offer a revolutionary approach to biomedical imaging, presenting a unique combination of high resolution, deep tissue penetration, and functional information. While challenges remain in ensuring biocompatibility, optimizing photoacoustic properties, and achieving high-resolution deep tissue imaging, the potential rewards are vast. With ongoing research efforts aimed at overcoming these challenges and exploring new opportunities, PA imaging nanoparticles are poised to transform the landscape of clinical diagnostics and therapeutic interventions.

Funding

This work was supported by Science and Engineering Research Board (SRG/2021/001465 & SUR/2022/001424); UGC-DAE consortium for scientific research (UGC-DAE-CRS/2021-22/02/513); SRM University AP internal research grants (SRMAP/URG/E&PP/2022-23/002 & SRMAP/URG/E&PP/2022-23/014) and National University of Singapore Resilience Growth Fund (A-0000065-99-99).

Data availability

Data will be made available on request.

CRediT authorship contribution statement

Pavan Mohan Neelamraju: Writing – original draft, Resources, Methodology, Data curation, Conceptualization. **Karthikay Gundepudi:** Writing – original draft, Methodology, Data curation, Conceptualization. **Pradyut Kumar Sanki:** Writing – original draft, Resources, Methodology. **Kumar Babu Busi:** Writing – original draft, Resources. **Tapan Kumar Mistri:** Writing – original draft, Resources, Methodology. **Sambasivam Sangaraju:** Writing – original draft, Resources. **Goutam Kumar Dalapati:** Writing – original draft, Resources, Funding acquisition. **Krishna Kanta Ghosh:** Writing – original draft, Resources. **Siddhartha Ghosh:** Writing – review & editing, Writing – original draft, Supervision, Resources, Project administration, Methodology, Funding acquisition, Data curation, Conceptualization. **Writoban Basu Ball:** Writing – original draft, Supervision, Resources, Project administration, Methodology. **Sabyasachi Chakrabortty:** Writing – review & editing, Writing – original draft, Supervision, Resources, Project administration, Methodology, Funding acquisition, Data curation, Conceptualization.

Declaration of competing interest

The authors declare that they have no known competing financial interests or personal relationships that could have appeared to influence the work reported in this paper.

References

[1] (a) Zishan Husain Khan, Mark Jackson, Numan A. Salah, Recent advances in nanomaterials, in: Springer Proceedings in Materials, Springer, 2023. PRINT ISBN: 978-981-99-4877-2;
(b) S.K. Kulkarni, Types of nanomaterials and their properties, in: S.K. Kulkarni (Ed.), BT -In: Nanotechnology: Principles and Practices, Springer International Publishing, Cham, 2015, pp. 199–239, https://doi.org/10.1007/978-3-319-09171-6_8. Print ISBN 978-3-319-09170-9;
(c) Bharat Bhushan, Dan Luo, Scott R. Schricker, Wolfgang Sigmund, Stefan Zauscher, Handbook of Nanomaterials Properties, Springer International Publishing, 2014, https://doi.org/10.1007/978-3-642-31107-9. ISBN 978-3-642-31106-2 ISBN 978-3-642-31107-9 (eBook);
(d) Mike Ashby, Paulo Ferreira, Daniel Schodek, Nanomaterials, in: Nanotechnolologies and Design: an Introduction for Engineers and Archiects, Butterworth-Heinemann ,Elsevier, 2009. ISBN: 978-0-7506-8149-0;
(e) Dieter Vollath, Nanomaterials - an introduction to synthesis, in: Properties, and Applications, second ed., WILEY-VCH, 2013. Print ISBN: 978-3-527-33379-0.

[2] D.F. Gardner, J.S. Evans, I.I. Smalyukh, Towards reconfigurable optical metamaterials: colloidal nanoparticle self-assembly and self-alignment in liquid crystals, Mol. Cryst. Liq. Cryst. 545 (2011) 3/[1227–21/[1245].

[3] (a) L. Zhai, A. Narkar, K. Ahn, Self-healing polymers with nanomaterials and nanostructures, Nano Today 30 (2020) 100826, https://doi.org/10.1016/j.nantod.2019.100826;
(b) C. Lutzweiler, D. Razansky, Optoacoustic imaging and tomography: reconstruction approaches and outstanding challenges in image performance and quantification, Sensors 13 (2013) 7345–7384;
(c) P. Beard, Biomedical photoacoustic imaging, Interface Focus 1 (2011) 602–631.

[4] A. Fatima, K. Kratkiewicz, R. Manwar, M. Zafar, R. Zhang, B. Huang, N. Dadashzadeh, J. Xia, K. Mohammad Avanaki, Review of cost reduction methods in photoacoustic computed tomography, Photoacoustics 15 (2019) 100137, https://doi.org/10.1016/j.pacs.2019.100137.

[5] W. David, Ball, an unusual form of spectroscopy uses light and sound to probe the behavior of materials, Here is a brief introduction to photoacoustic spectroscopy 21 (2006) 14–16.

[6] S. Mallidi, E. Yantsen, T. Larson, K. Sokolov, S. Emelianov, Molecular specific photoacoustic imaging with plasmonic nanosensors, in: Proc.SPIE, 2008 685616, https://doi.org/10.1117/12.763903.

[7] R.A. Kruger, Photoacoustic ultrasound, Med. Phys. 21 (1994) 127–131, https://doi.org/10.1118/1.597367.

[8] A. Agarwal, S.W. Huang, M. O'Donnell, K.C. Day, M. Day, N. Kotov, S. Ashkenazi, Targeted gold nanorod contrast agent for prostate cancer detection by photoacoustic imaging, J. Appl. Phys. 102 (2007) 64701, https://doi.org/10.1063/1.2777127.

[9] V. Koskinen, J. Fonsen, K. Roth, J. Kauppinen, Progress in cantilever enhanced photoacoustic spectroscopy, Vib. Spectrosc. 48 (2008) 16–21, https://doi.org/10.1016/j.vibspec.2008.01.013.

[10] W. Smith, The action of light on selenium, J. Soc. Telegr. Eng. 2 (n.d.) 31–33. https://api.semanticscholar.org/CorpusID:137216883.

[11] A.G. Bell, Oeiginal Communications, Upon the Production and Reproduction of Sound by Light, 1880, pp. 404–426.

[12] Selenium and the Photophone1, Nature. 22 (1880) 500–503. https://doi.org/10.1038/022500a0.

[13] W.H. Preece, W. Spottiswoode, I. On the conversion of radiant energy into sonorous vibrations, Proc. R. Soc. London, A 31 (1997) 506–520, https://doi.org/10.1098/rspl.1880.0071.

[14] J. Tyndall III, Action of an intermittent beam of radiant heat upon gaseous matter, Proc. R. Soc. London, A 31 (1997) 307–317, https://doi.org/10.1098/rspl.1880.0037.

[15] A.G. Bell, The production of sound by radiant energy, Science os-2 (1881) 242–253, https://doi.org/10.1126/science.os-2.48.242.

[16] M.E. Gorman, Alexander Graham Bell 1847–1922, Encycl. Creat XXIII (2011) e1–e2, https://doi.org/10.1016/b978-0-12-375038-9.00026-1.

[17] RAYLEIGH, The Photophone, Nature. 23 (1881) 274–275. https://doi.org/10.1038/023274a0.

[18] E. Mercadier, Sur la radiophonie, J. Phys. Theor. Appl. 10 (1881) 53–68. https://doi.org/10.1051/jphystap:018810010005300.

[19] E. Mercadier, Sur la radiophonie (2e mémoire), J. Phys. Theor. Appl. 10 (1881) 147–154. https://doi.org/10.1051/jphystap:0188100100014701.

[20] T. Param, P. Specimens, A Nn . Aì, 2004, pp. 1–13.

[21] S. of T.E. and Electricians, Journal of the Society of Telegraph Engineers and of Electricians: including original communications on telegraphy and electrical science 8 (1881) file://catalog.hathitrust.org/Record/008896842.

[22] A.O. Rankine, On the transmission of speech by light, Proc. Phys. Soc., London 31 (1918) 242, https://doi.org/10.1088/1478-7814/31/1/325.

[23] A.H. Pfund, Atmospheric contamination, Science 90 (1939) 326–327, https://doi.org/10.1126/science.90.2336.326.

[24] S. Manohar, D. Razansky, Photoacoustics: a historical review, Adv. Opt. Photonics 8 (2016) 586–617, https://doi.org/10.1364/AOP.8.000586.

[25] M. Vengerov, An optical-acoustic method of gas analysis, Nature 158 (1946) 28–29, https://doi.org/10.1038/158028c0.

[26] Z. Hosseinaee, M. Le, K. Bell, P.H. Reza, Towards non-contact photoacoustic imaging, Photoacoustics 20 (2020) 100207, https://doi.org/10.1016/j.pacs.2020.100207 [review].

[27] A. Blohm, A. Sieburg, J. Popp, T. Frosch, 6 - detection of gas molecules by means of spectrometric and spectroscopic methods, in: L. Baia, Z. Pap, K. Hernadi, E. H. Baia (Eds.), Micro Nano Technol, Elsevier, 2020, pp. 251–294, https://doi.org/10.1016/B978-0-12-815882-1.00006-9.

[28] Y. Cai, N. Arsad, M. Li, Y. Wang, Buffer structure optimization of the photoacoustic cell for trace gas detection, Optoelectron. Lett. 9 (2013) 233–237, https://doi.org/10.1007/s11801-013-3017-3.

[29] S. Wang, L. Fu, J. Xin, S. Wang, C. Yao, Z. Zhang, J. Wang, Photoacoustic response induced by nanoparticle-mediated photothermal bubbles beyond the thermal expansion for potential theranostics, J. Biomed. Opt. 23 (2018) 1, https://doi.org/10.1117/1.jbo.23.12.125002.

[30] H. Liu, H. Zhang, J. Wang, J. Wei, Effect of temperature on the size of biosynthesized silver nanoparticle: deep insight into microscopic kinetics analysis, Arab. J. Chem. 13 (2020) 1011–1019, https://doi.org/10.1016/j.arabjc.2017.09.004.

[31] R.C. Gray, A.J. Bard, Photoacoustic spectroscopy applied to systems involving photoinduced gas evolution or consumption, Anal. Chem. 50 (1978) 1262–1265, https://doi.org/10.1021/ac50031a018.

[32] D. Wróbel, A. Graja, Modification of electronic structure in supramolecular fullerene–porphyrin systems studied by fluorescence, photoacoustic and photothermal spectroscopy, J. Photochem. Photobiol. Chem. 183 (2006) 79–88, https://doi.org/10.1016/j.jphotochem.2006.02.024.

[33] G. Bults, B.A. Horwitz, S. Malkin, D. Cahen, Photoacoustic measurements of photosynthetic activities in whole leaves. Photochemistry and gas exchange, Biochim. Biophys. Acta Bioenerg. 679 (1982) 452–465, https://doi.org/10.1016/0005-2728(82)90167-0.

[34] D. Balasubramanian, C.H.M. Rao, Biological applications of photoacoustic spectroscopy, Curr. Sci. 51 (1982) 111–117. http://www.jstor.org/stable/24086176.

[35] J. Kolbowski, H. Reising, U. Schreiber, Computer-controlled pulse modulation system for analysis of photoacoustic signals in the time domain, Photosynth. Res. 25 (1990) 309–316, https://doi.org/10.1007/BF00033172.

[36] M. Erfanzadeh, Q. Zhu, Photoacoustic imaging with low-cost sources; A review, Photoacoustics 14 (2019) 1–11, https://doi.org/10.1016/j.pacs.2019.01.004.

[37] J.T. Friedlein, E. Baumann, K.A. Briggman, G.M. Colacion, F.R. Giorgetta, A.M. Goldfain, D.I. Herman, E.V. Hoenig, J. Hwang, N.R. Newbury, E.F. Perez, C. S. Yung, I. Coddingto, K.C. Cossel, Dual-comb photoacoustic spectroscopy, Nat. Commun. 11 (2020) 3152, https://doi.org/10.1038/s41467-020-16917-y.

[38] Dependence of the Michelson interferometer-based membrane-less optical microphone–photoacoustic spectroscopy gas-sensing method on the fundamental parameters of a photoacoustic gas cell, Photonics 10 (8) (2023) 888, https://doi.org/10.3390/photonics10080888.

[39] T.D. Le, S.Y. Kwon, C. Lee, Segmentation and quantitative analysis of photoacoustic imaging: a review, Photonics 9 (3) (2022) 176, https://doi.org/10.3390/photonics9030176.

[40] Jens Buchmann, Bernhard Kaplan, Samuel Powell, Steffen Prohaska, Jan Laufer, Quantitative PA tomography of high resolution 3-D images: experimental validation in a tissue phantom, Photoacoustics 17 (2020) 100157, https://doi.org/10.1016/j.pacs.2019.100157.

[41] R. Manwar, M. Zafar, Q. Xu, Signal and image processing in biomedical photoacoustic imaging, A Review, Optics 2 (2021) 1–24, https://doi.org/10.3390/opt2010001.

[42] A. Da Silva, C. Handschin, K. Metwally, H. Garci, C. Riedinger, S. Mensah, H. Akhouayri, Taking advantage of acoustic inhomogeneities in photoacoustic measurements, J. Biomed. Opt. 22 (2017) 41012, https://doi.org/10.1117/1.JBO.22.4.041012.

[43] M. Havaux, Photoacoustic study of the photochemical energy conversion in Epilobium plants grown under very low light conditions, Environ. Exp. Bot. 30 (1990) 101–109, https://doi.org/10.1016/0098-8472(90)90014-U.

[44] S. Malkin, D. Cahln, Photoacoustic spectroscopy and radiant energy conversion: theory of the effect with special emphasis on photosynthesis, Photochem. Photobiol. 29 (1979) 803–813, https://doi.org/10.1111/j.1751-1097.1979.tb07770.x.

[45] D. Cahen, Photoacoustic determination of photovoltaic energy conversion efficiency, Appl. Phys. Lett. 33 (2008) 810–811, https://doi.org/10.1063/1.90536.

[46] P. Liu, Photoacoustic energy conversion efficiency for a simplified absorber model, in: Soc. Photo-Optical Instrum. Eng. Conf. Ser., AA(Indiana Univ. School of Medicine), 1994, pp. 89–92. https://ui.adsabs.harvard.edu/abs/1994SPIE.2134A..89L.

[47] B. Büchner, H.W. Schock, Photothermal characterization of materials suitable for thin film solar cells, in: D. Bićanić (Ed.), BT - Photoacoustic and Photothermal Phenomena III, Springer Berlin Heidelberg, Berlin, Heidelberg, 1992, pp. 406–407.

[48] L. Li, A.A. Shemetov, M. Baloban, P. Hu, L. Zhu, D.M. Shcherbakova, R. Zhang, J. Shi, J. Yao, L. V Wang, V. V Verkhusha, Small near-infrared photochromic protein for photoacoustic multi-contrast imaging and detection of protein interactions in vivo, Nat. Commun. 9 (2018) 2734, https://doi.org/10.1038/s41467-018-05231-3.

[49] D. Kumar, D. Ghai, R. Soni, Simulation studies of photoacoustic response from gold-silica core-shell nanoparticles, Plasmonics 13 (2018), https://doi.org/10.1007/s11468-018-0697-3.

[50] Y.-S. Chen, W. Frey, S. Aglyamov, S. Emelianov, Environment-dependent generation of photoacoustic waves from plasmonic nanoparticles, Small 8 (2012) 47–52, https://doi.org/10.1002/smll.201101140.

[51] M. Pramanik Verawaty, Simulating photoacoustic waves from individual nanoparticle of various shapes using k-Wave, Biomed, Phys. Eng. Express. 2 (2016) 35013, https://doi.org/10.1088/2057-1976/2/3/035013.

[52] W. Li, X. Chen, Gold nanoparticles for photoacoustic imaging, Nanomedicine 10 (2015) 299–320, https://doi.org/10.2217/nnm.14.169.

[53] I. Khan, K. Saeed, I. Khan, Nanoparticles: properties, applications and toxicities, Arab. J. Chem. 12 (2019) 908–931, https://doi.org/10.1016/j.arabjc.2017.05.011.

[54] D. Kumar, R.K. Soni, D.P. Ghai, Pulsed photoacoustic and photothermal response of gold nanoparticles, Nanotechnology 31 (2020) 35704, https://doi.org/10.1088/1361-6528/ab47ae.

[55] G. Wang, F. Zhang, R. Tian, L. Zhang, G. Fu, L. Yang, L. Zhu, Nanotubes-embedded indocyanine green–hyaluronic acid nanoparticles for photoacoustic-imaging-guided phototherapy, ACS Appl. Mater. Interfaces 8 (2016) 5608–5617, https://doi.org/10.1021/acsami.5b12400.

[56] S. Han, R. Bouchard, K. V Sokolov, Molecular photoacoustic imaging with ultra-small gold nanoparticles, Biomed. Opt Express 10 (2019) 3472–3483, https://doi.org/10.1364/BOE.10.003472.

[57] A. Sheinfeld, W.J. Eldridge, A. Wax, Quantitative phase imaging with molecular sensitivity using photoacoustic microscopy with a miniature ring transducer, J. Biomed. Opt. 20 (2015) 86002, https://doi.org/10.1117/1.JBO.20.8.086002.

[58] Q. Fu, R. Zhu, J. Song, H. Yang, X. Chen, Photoacoustic imaging: contrast agents and their biomedical applications, Adv. Mater. 31 (2019) 1805875, https://doi.org/10.1002/adma.201805875.

[59] J. Weber, P.C. Beard, S.E. Bohndiek, Contrast agents for molecular photoacoustic imaging, Nat. Methods 13 (2016) 639–650, https://doi.org/10.1038/nmeth.3929.

[60] C.L. Bayer, Y.-S. Chen, S. Kim, S. Mallidi, K. Sokolov, S. Emelianov, Multiplex photoacoustic molecular imaging using targeted silica-coated gold nanorods, Biomed. Opt Express 2 (2011) 1828–1835, https://doi.org/10.1364/BOE.2.001828.

[61] M. Mehrmohammadi, S.J. Yoon, D. Yeager, S.Y. Emelianov, Photoacoustic imaging for cancer detection and staging, Curr. Mol. Imag. 2 (2013) 89–105, https://doi.org/10.2174/2211555211302010010.

[62] A.B. Asha, R. Narain, in: R.B. TPS, N. Narain (Eds.), Chapter 15 - Nanomaterials Properties, Elsevier, 2020, pp. 343–359, https://doi.org/10.1016/B978-0-12-816806-6.00015-7.

[63] X. Yang, E.W. Stein, S. Ashkenazi, L. V Wang, Nanoparticles for photoacoustic imaging, WIREs Nanomedicine and Nanobiotechnology 1 (2009) 360–368, https://doi.org/10.1002/wnan.42.

[64] P.K. Jain, K.S. Lee, I.H. El-Sayed, M.A. El-Sayed, Calculated absorption and scattering properties of gold nanoparticles of different size, shape, and composition: applications in biological imaging and biomedicine, J. Phys. Chem. B 110 (2006) 7238–7248, https://doi.org/10.1021/jp057170o.

[65] R. Liu, J. Tang, Y. Xu, Y. Zhou, Z. Dai, Nano-sized indocyanine green J-aggregate as a one-component theranostic agent, Nanotheranostics 1 (2017) 430–439, https://doi.org/10.7150/ntno.19935.

[66] H.K. Yoon, A. Ray, Y.-E. Koo Lee, G. Kim, X. Wang, R. Kopelman, Polymer–protein hydrogel nanomatrix for stabilization of indocyanine green towards targeted fluorescence and photoacoustic bio-imaging, J. Mater. Chem. B 1 (2013) 5611–5619, https://doi.org/10.1039/C3TB21060J.

[67] Y. Zhang, M. Jeon, L.J. Rich, H. Hong, J. Geng, Y. Zhang, S. Shi, T.E. Barnhart, P. Alexandridis, J.D. Huizinga, M. Seshadri, W. Cai, C. Kim, J.F. Lovell, Non-invasive multimodal functional imaging of the intestine with frozen micellar naphthalocyanines, Nat. Nanotechnol. 9 (2014) 631–638, https://doi.org/10.1038/nnano.2014.130.

[68] K.M. Harmatys, J. Chen, D.M. Charron, C.M. MacLaughlin, G. Zheng, Multipronged biomimetic approach to create optically tunable nanoparticles, Angew. Chem., Int. Ed. Engl. 57 (2018) 8125–8129, https://doi.org/10.1002/anie.201803535.

[69] I.C. Sun, D.S. Dumani, S.Y. Emelianov, Applications of the photocatalytic and photoacoustic properties of gold nanorods in contrast-enhanced ultrasound and photoacoustic imaging, ACS Nano 18 (4) (2024) 3575–3582, https://doi.org/10.1021/acsnano.3c11223.

[70] K. Cai, W. Zhang, M.d F. Foda, X. Li, J. Zhang, Y. Zhong, H. Liang, H. Li, H. Han, T. Zhai, Miniature hollow gold nanorods with enhanced effect for in vivo photoacoustic imaging in the NIR-II window, Small 16 (37) (2020), https://doi.org/10.1002/smll.202002748.

[71] G.P. Luke, J.N. Myers, S.Y. Emelianov, K. V Sokolov, Sentinel lymph node biopsy revisited: ultrasound-guided photoacoustic detection of micrometastases using molecularly targeted plasmonic nanosensors, Cancer Res. 74 (2014) 5397–5408, https://doi.org/10.1158/0008-5472.CAN-14-0796.

[72] C. Bao, J. Conde, F. Pan, C. Li, C. Zhang, F. Tian, S. Liang, J.M. de la Fuente, D. Cui, Gold nanoprisms as a hybrid in vivo cancer theranostic platform for in situ photoacoustic imaging, angiography, and localized hyperthermia, Nano Res. 9 (2016) 1043–1056, https://doi.org/10.1007/s12274-016-0996-y.

[73] Y. Zhao, W. Liu, Y. Tian, Z. Yang, X. Wang, Y. Zhang, Y. Tang, S. Zhao, C. Wang, Y. Liu, J. Sun, Z. Teng, S. Wang, G. Lu, Anti-EGFR peptide-conjugated triangular gold nanoplates for computed tomography/photoacoustic imaging-guided photothermal therapy of non-small cell lung cancer, ACS Appl. Mater. Interfaces 10 (2018) 16992–17003, https://doi.org/10.1021/acsami.7b19013.

[74] K.B. Busi, S. Das, M. Palanivel, K.K. Ghosh, B. Gulyás, P. Padmanabhan, S. Chakrabortty, Surface ligand influences the Cu nanoclusters as a dual sensing optical probe for localized pH environment and fluoride ion, Nanomaterials 13 (2023), https://doi.org/10.3390/nano13030529.

[75] H. Soo Choi, W. Liu, P. Misra, E. Tanaka, J.P. Zimmer, B. Itty Ipe, M.G. Bawendi, J. V Frangioni, Renal clearance of quantum dots, Nat. Biotechnol. 25 (2007) 1165–1170, https://doi.org/10.1038/nbt1340.

[76] M. Yu, J. Xu, J. Zheng, Renal clearable luminescent gold nanoparticles: from the bench to the clinic, Angew. Chem. Int. Ed. 58 (2019) 4112–4128, https://doi.org/10.1002/anie.201807847.

[77] F. Chen, K. Ma, B. Madajewski, L. Zhuang, L. Zhang, K. Rickert, M. Marelli, B. Yoo, M.Z. Turker, M. Overholtzer, T.P. Quinn, M. Gonen, P. Zanzonico, A. Tuesca, M.A. Bowen, L. Norton, J.A. Subramony, U. Wiesner, M.S. Bradbury, Ultrasmall targeted nanoparticles with engineered antibody fragments for imaging detection of HER2-overexpressing breast cancer, Nat. Commun. 9 (2018) 4141, https://doi.org/10.1038/s41467-018-06271-5.

[78] B. Du, M. Yu, J. Zheng, Transport and interactions of nanoparticles in the kidneys, Nat. Rev. Mater. 3 (2018) 358–374, https://doi.org/10.1038/s41578-018-0038-3.

[79] C. Buzea, I.I. Pacheco, K. Robbie, Nanomaterials and nanoparticles: sources and toxicity, Biointerphases 2 (2007) MR17–71, https://doi.org/10.1116/1.2815690.

[80] H.H. Gustafson, D. Holt-Casper, D.W. Grainger, H. Ghandehari, Nanoparticle uptake: the phagocyte problem, Nano Today 10 (2015) 487–510, https://doi.org/10.1016/j.nantod.2015.06.006.

[81] C.L. Bayer, G.P. Luke, S.Y. Emelianov, Photoacoustic imaging for medical diagnostics, Acoust. Today 8 (2012) 15–23, https://doi.org/10.1121/1.4788648.

[82] M.G. González, X. Liu, R. Niessner, C. Haisch, Strong size-dependent photoacoustic effect on gold nanoparticles by laser-induced nanobubbles, Appl. Phys. Lett. 96 (2010) 174104, https://doi.org/10.1063/1.3387890.

[83] X. Yu, A. Li, C. Zhao, K. Yang, X. Chen, W. Li, Ultrasmall semimetal nanoparticles of bismuth for dual-modal computed tomography/photoacoustic imaging and synergistic thermoradiotherapy, ACS Nano 11 (2017) 3990–4001, https://doi.org/10.1021/acsnano.7b00476.

[84] T.A. El-Brolossy, T. Abdallah, M.B. Mohamed, S. Abdallah, K. Easawi, S. Negm, H. Talaat, Shape and size dependence of the surface plasmon resonance of gold nanoparticles studied by Photoacoustic technique, Eur. Phys. J. Spec. Top. 153 (2008) 361–364, https://doi.org/10.1140/epjst/e2008-00462-0.

[85] A. Hatef, B. Darvish, A. Dagallier, Y.R. Davletshin, W. Johnston, J.C. Kumaradas, D. Rioux, M. Meunier, Analysis of photoacoustic response from gold–silver alloy nanoparticles irradiated by short pulsed laser in water, J. Phys. Chem. C 119 (2015) 24075–24080, https://doi.org/10.1021/acs.jpcc.5b08359.

[86] W. Yim, J. Zhou, Y. Mantri, M.N. Creyer, C.A. Moore, J. V Jokerst, Gold nanorod–melanin hybrids for enhanced and prolonged photoacoustic imaging in the near-infrared-II window, ACS Appl. Mater. Interfaces 13 (2021) 14974–14984, https://doi.org/10.1021/acsami.1c00993.
[87] T. Repenko, A. Rix, A. Nedilko, J. Rose, A. Hermann, R. Vinokur, S. Moli, R. Cao-Milàn, M. Mayer, G. von Plessen, A. Fery, L. De Laporte, W. Lederle, D. N. Chigrin, A.J.C. Kuehne, Strong photoacoustic signal enhancement by coating gold nanoparticles with melanin for biomedical imaging, Adv. Funct. Mater. 28 (2018) 1705607, https://doi.org/10.1002/adfm.201705607.
[88] Front Matter, in: Nanotechnol. Biomed. Imaging Diagnostics, 2014, pp. i–xix, https://doi.org/10.1002/9781118873151.fmatter.
[89] M.Y. Berezin, Historical perspective on nanoparticles in imaging from 1895 to 2000, in: Nanotechnol. Biomed. Imaging Diagnostics, 2014, pp. 1–23, https://doi.org/10.1002/9781118873151.ch1.
[90] S. Zhang, S. Sun, Iron oxide-based magnetic nanoparticles synthesized from the organic solution phase for advanced biological imaging, in: Nanotechnol. Biomed. Imaging Diagnostics, 2014, pp. 25–48, https://doi.org/10.1002/9781118873151.ch2.
[91] T. Elbayoumi, V. Torchilin, Lipid-based pharmaceutical nanocarriers for imaging applications, in: Nanotechnol. Biomed. Imaging Diagnostics, 2014, pp. 49–81, https://doi.org/10.1002/9781118873151.ch3.
[92] S.A. Dergunov, E. Pinkhassik, Hollow nanocapsules in biomedical imaging applications, in: Nanotechnol. Biomed. Imaging Diagnostics, 2014, pp. 83–109, https://doi.org/10.1002/9781118873151.ch4.
[93] A. V Liopo, A.A. Oraevsky, Nanoparticles as contrast agents for optoacoustic imaging, in: Nanotechnol. Biomed. Imaging Diagnostics, 2014, pp. 111–149, https://doi.org/10.1002/9781118873151.ch5.
[94] K. Nelson, P. Winter, M. Shokeen, S. Wang, M.Y. Berezin, Nanoparticles for bioimaging, in: Nanotechnol. Biomed. Imaging Diagnostics, 2014, pp. 151–192, https://doi.org/10.1002/9781118873151.ch6.
[95] T. Aweda, D. Sultan, Y. Liu, Radio-labeled nanoparticles for biomedical imaging, in: Nanotechnol. Biomed. Imaging Diagnostics, 2014, pp. 193–221, https://doi.org/10.1002/9781118873151.ch7.
[96] F. Guérard, G.L. Ray, M.W. Brechbiel, MRI with gadolinium-based nanoparticles, in: Nanotechnol. Biomed. Imaging Diagnostics, 2014, pp. 223–262, https://doi.org/10.1002/9781118873151.ch8.
[97] Y. Ardeshirpour, V. Chernomordik, M. Hassan, A.H. Gandjbakhche, D. Sackett, In vivo molecular fluorescence imaging, in: Nanotechnol. Biomed. Imaging Diagnostics, 2014, pp. 263–292, https://doi.org/10.1002/9781118873151.ch9.
[98] M. Jeon, C. Kim, Photoacoustic and ultrasound imaging with nanosized contrast agents, in: Nanotechnol. Biomed. Imaging Diagnostics, 2014, pp. 293–323, https://doi.org/10.1002/9781118873151.ch10.
[99] L. Tian, S. Singamaneni, Surface-enhanced Raman scattering-based bioimaging, in: Nanotechnol. Biomed. Imaging Diagnostics, 2014, pp. 325–346, https://doi.org/10.1002/9781118873151.ch11.
[100] C. Schoen, C. London, Pandia®, in: Nanotechnol. Biomed. Imaging Diagnostics, 2014, pp. 347–372, https://doi.org/10.1002/9781118873151.ch12.
[101] J.-S. Taylor, Imaging genetic information, in: Nanotechnol. Biomed. Imaging Diagnostics, 2014, pp. 373–400, https://doi.org/10.1002/9781118873151.ch13.
[102] A.M. Wen, C.-F. Cho, J.D. Lewis, N.F. Steinmetz, The application of plant viral nanoparticles in tissue-specific imaging, in: Nanotechnol. Biomed. Imaging Diagnostics, 2014, pp. 401–427, https://doi.org/10.1002/9781118873151.ch14.
[103] J.M. Janjic, M. Bai, Design and development of theranostic nanomedicines, in: Nanotechnol. Biomed. Imaging Diagnostics, 2014, pp. 429–465, https://doi.org/10.1002/9781118873151.ch15.
[104] G. Talcott, W.J. Akers, Animal models for preclinical imaging, in: Nanotechnol. Biomed. Imaging Diagnostics, 2014, pp. 467–486, https://doi.org/10.1002/9781118873151.ch16.
[105] D. Pan, M. Pramanik, S.A. Wickline, L. V Wang, G.M. Lanza, Recent advances in colloidal gold nanobeacons for molecular photoacoustic imaging, Contrast Media Mol. Imaging 6 (2011) 378–388, https://doi.org/10.1002/cmmi.449.
[106] L.R. Hirsch, R.J. Stafford, J.A. Bankson, S.R. Sershen, B. Rivera, R.E. Price, J.D. Hazle, N.J. Halas, J.L. West, Nanoshell-mediated near-infrared thermal therapy of tumors under magnetic resonance guidance, Proc. Natl. Acad. Sci. USA 100 (2003) 13549–13554, https://doi.org/10.1073/pnas.2232479100.
[107] M. Sun, F. Liu, Y. Zhu, W. Wang, J. Hu, J. Liu, Z. Dai, K. Wang, Y. Wei, J. Bai, W. Gao, Salt-induced aggregation of gold nanoparticles for photoacoustic imaging and photothermal therapy of cancer, Nanoscale 8 (2016) 4452–4457, https://doi.org/10.1039/C6NR00056H.
[108] M.A. Valverde-Alva, T. García-Fernández, M. Villagrán-Muniz, C. Sánchez-Aké, R. Castañeda-Guzmán, E. Esparza-Alegría, C.F. Sánchez-Valdés, J.L. S. Llamazares, C.E.M. Herrera, Synthesis of silver nanoparticles by laser ablation in ethanol: a pulsed photoacoustic study, Appl. Surf. Sci. 355 (2015) 341–349, https://doi.org/10.1016/j.apsusc.2015.07.133.
[109] J.J. Mock, M. Barbic, D.R. Smith, D.A. Schultz, S. Schultz, Shape effects in plasmon resonance of individual colloidal silver nanoparticles, J. Chem. Phys. 116 (2002) 6755–6759, https://doi.org/10.1063/1.1462610.
[110] D. Chen, X. Qiao, X. Qiu, J. Chen, Synthesis and electrical properties of uniform silver nanoparticles for electronic applications, J. Mater. Sci. 44 (2009) 1076–1081, https://doi.org/10.1007/s10853-008-3204-y.
[111] Y. Lyu, Y. Fang, Q. Miao, X. Zhen, D. Ding, K. Pu, Intraparticle molecular orbital engineering of semiconducting polymer nanoparticles as amplified theranostics for in vivo photoacoustic imaging and photothermal therapy, ACS Nano 10 (2016) 4472–4481, https://doi.org/10.1021/acsnano.6b00168.
[112] B. Silvestri, P. Armanetti, G. Sanità, G. Vitiello, A. Lamberti, G. Calì, A. Pezzella, G. Luciani, L. Menichetti, S. Luin, M. d'Ischia, Silver-nanoparticles as plasmon-resonant enhancers for eumelanin's photoacoustic signal in a self-structured hybrid nanoprobe, Mater. Sci. Eng. C 102 (2019) 788–797, https://doi.org/10.1016/j.msec.2019.04.066.
[113] Z. Xiu, Q. Zhang, H.L. Puppala, V.L. Colvin, P.J.J. Alvarez, Negligible particle-specific antibacterial activity of silver nanoparticles, Nano Lett. 12 (2012) 4271–4275, https://doi.org/10.1021/nl301934w.
[114] T. Kim, Q. Zhang, J. Li, L. Zhang, J. V Jokerst, A gold/silver hybrid nanoparticle for treatment and photoacoustic imaging of bacterial infection, ACS Nano 12 (2018) 5615–5625, https://doi.org/10.1021/acsnano.8b01362.
[115] T.M.T. Vo, S. Mondal, V.T. Nguyen, S. Park, J. Choi, N.T. Bui, J. Oh, Rice starch coated iron oxide nanoparticles: a theranostic probe for photoacoustic imaging-guided photothermal cancer therapy, Int. J. Biol. Macromol. 183 (2021) 55–67, https://doi.org/10.1016/j.ijbiomac.2021.04.053.
[116] R. Zhang, Q. Fan, M. Yang, K. Cheng, X. Lu, L. Zhang, W. Huang, Z. Cheng, Engineering melanin nanoparticles as an efficient drug-delivery system for imaging-guided chemotherapy, Adv. Mater. 27 (2015) 5063–5069, https://doi.org/10.1002/adma.201502201.
[117] K.-Y. Ju, J.W. Lee, G.H. Im, S. Lee, J. Pyo, S.B. Park, J.H. Lee, J.-K. Lee, Bio-inspired, melanin-like nanoparticles as a highly efficient contrast agent for T1-weighted magnetic resonance imaging, Biomacromolecules 14 (2013) 3491–3497, https://doi.org/10.1021/bm4008138.
[118] J.E. Lemaster, Z. Wang, A. Hariri, F. Chen, Z. Hu, Y. Huang, C. V Barback, R. Cochran, N.C. Gianneschi, J. V Jokerst, Gadolinium doping enhances the photoacoustic signal of synthetic melanin nanoparticles: a dual modality contrast agent for stem cell imaging, Chem. Mater. 31 (2019) 251–259, https://doi.org/10.1021/acs.chemmater.8b04333.
[119] G. Ku, M. Zhou, S. Song, Q. Huang, J. Hazle, C. Li, Copper sulfide nanoparticles as a new class of photoacoustic contrast agent for deep tissue imaging at 1064 nm, ACS Nano 6 (2012) 7489–7496, https://doi.org/10.1021/nn302782y.
[120] Y.-S. Ko, Y.H. Joe, M. Seo, K. Lim, J. Hwang, K. Woo, Prompt and synergistic antibacterial activity of silver nanoparticle-decorated silica hybrid particles on air filtration, J. Mater. Chem. B 2 (2014) 6714–6722, https://doi.org/10.1039/C4TB01068J.
[121] Y. Li, W. Lu, Q. Huang, M. Huang, C. Li, W. Chen, Copper sulfide nanoparticles for photothermal ablation of tumor cells, Nanomedicine 5 (2010) 1161–1171, https://doi.org/10.2217/nnm.10.85.
[122] M. Zhou, R. Zhang, M. Huang, W. Lu, S. Song, M.P. Melancon, M. Tian, D. Liang, C. Li, A chelator-free multifunctional [64Cu]CuS nanoparticle platform for simultaneous micro-PET/CT imaging and photothermal ablation therapy, J. Am. Chem. Soc. 132 (2010) 15351–15358, https://doi.org/10.1021/ja106855m.
[123] A.M.S. Krishna, B. Ramasubramanian, S. Haseena, P. Bamola, H. Sharma, C. Mahata, A. Chroneos, S. Krishnamurthy, M.K. Ravva, B. Chandu, Y.F. Lim, A. Kumar, S. Ramakrishna, S. Biring, S. Chakrabortty, G.K. Dalapati, Functionalized graphene-incorporated cupric oxide charge-transport layer for enhanced photoelectrochemical performance and hydrogen evolution, Catalysts 13 (2023), https://doi.org/10.3390/catal13040785.

[124] B. Park, K.M. Lee, S. Park, M. Yun, H.-J. Choi, J. Kim, C. Lee, H. Kim, C. Kim, Deep tissue photoacoustic imaging of nickel(II) dithiolene-containing polymeric nanoparticles in the second near-infrared window, Theranostics 10 (2020) 2509–2521, https://doi.org/10.7150/thno.39403.
[125] J. Koo, M. Jeon, Y. Oh, H.W. Kang, J. Kim, C. Kim, J. Oh, In vivo non-ionizing photoacoustic mapping of sentinel lymph nodes and bladders with ICG-enhanced carbon nanotubes, Phys. Med. Biol. 57 (2012) 7853–7862, https://doi.org/10.1088/0031-9155/57/23/7853.
[126] C. Kim, M. Jeon, L. V Wang, Nonionizing photoacoustic cystography in vivo, Opt. Lett. 36 (2011) 3599–3601, https://doi.org/10.1364/OL.36.003599.
[127] G. Song, Q. Wang, Y. Wang, G. Lv, C. Li, R. Zou, Z. Chen, Z. Qin, K. Huo, R. Hu, J. Hu, A low-toxic multifunctional nanoplatform based on Cu9S5@mSiO2 core-shell nanocomposites: combining photothermal- and chemotherapies with infrared thermal imaging for cancer treatment, Adv. Funct. Mater. 23 (2013) 4281–4292, https://doi.org/10.1002/adfm.201203317.
[128] Y. Cai, P. Liang, Q. Tang, X. Yang, W. Si, W. Huang, Q. Zhang, X. Dong, Diketopyrrolopyrrole–triphenylamine organic nanoparticles as multifunctional reagents for photoacoustic imaging-guided photodynamic/photothermal synergistic tumor therapy, ACS Nano 11 (2017) 1054–1063, https://doi.org/10.1021/acsnano.6b07927.
[129] K. Gao, W. Tu, X. Yu, F. Ahmad, X. Zhang, W. Wu, X. An, X. Chen, W. Li, W-doped TiO(2) nanoparticles with strong absorption in the NIR-II window for photoacoustic/CT dual-modal imaging and synergistic thermoradiotherapy of tumors, Theranostics 9 (2019) 5214–5226, https://doi.org/10.7150/thno.33574.
[130] Y. Jiang, K. Pu, Advanced photoacoustic imaging applications of near-infrared absorbing organic nanoparticles, Small 13 (2017) 1700710, https://doi.org/10.1002/smll.201700710.
[131] L. V Wang, S. Hu, Photoacoustic tomography: in vivo imaging from organelles to organs, Science 335 (2012) 1458–1462, https://doi.org/10.1126/science.1216210.
[132] Q. Fan, K. Cheng, Z. Yang, R. Zhang, M. Yang, X. Hu, X. Ma, L. Bu, X. Lu, X. Xiong, W. Huang, H. Zhao, Z. Cheng, Perylene-diimide-based nanoparticles as highly efficient photoacoustic agents for deep brain tumor imaging in living mice, Adv. Mater. 27 (2015) 843–847, https://doi.org/10.1002/adma.201402972.
[133] X. Zheng, L. Wang, S. Liu, W. Zhang, F. Liu, Z. Xie, Nanoparticles of chlorin dimer with enhanced absorbance for photoacoustic imaging and phototherapy, Adv. Funct. Mater. 28 (2018) 1706507, https://doi.org/10.1002/adfm.201706507.
[134] W. Zhang, W. Lin, Q. Pei, X. Hu, Z. Xie, X. Jing, Redox-hypersensitive organic nanoparticles for selective treatment of cancer cells, Chem. Mater. 28 (2016) 4440–4446, https://doi.org/10.1021/acs.chemmater.6b01641.
[135] J. Liu, J. Geng, L.-D. Liao, N. Thakor, X. Gao, B. Liu, Conjugated polymer nanoparticles for photoacoustic vascular imaging, Polym. Chem. 5 (2014) 2854–2862, https://doi.org/10.1039/C3PY01587D.
[136] K. Li, B. Liu, Polymer-encapsulated organic nanoparticles for fluorescence and photoacoustic imaging, Chem. Soc. Rev. 43 (2014) 6570–6597, https://doi.org/10.1039/C4CS00014E.
[137] L. Cheng, K. Yang, Q. Chen, Z. Liu, Organic stealth nanoparticles for highly effective in vivo near-infrared photothermal therapy of cancer, ACS Nano 6 (2012) 5605–5613, https://doi.org/10.1021/nn301539m.
[138] J. V Jokerst, D. Van de Sompel, S.E. Bohndiek, S.S. Gambhir, Cellulose nanoparticles are a biodegradable photoacoustic contrast agent for use in living mice, Photoacoustics 2 (2014) 119–127, https://doi.org/10.1016/j.pacs.2014.07.001.
[139] Z. Zha, X. Yue, Q. Ren, Z. Dai, Uniform polypyrrole nanoparticles with high photothermal conversion efficiency for photothermal ablation of cancer cells, Adv. Mater. 25 (2013) 777–782, https://doi.org/10.1002/adma.201202211.
[140] K. Yang, H. Xu, L. Cheng, C. Sun, J. Wang, Z. Liu, In vitro and in vivo near-infrared photothermal therapy of cancer using polypyrrole organic nanoparticles, Adv. Mater. 24 (2012) 5586–5592, https://doi.org/10.1002/adma.201202625.
[141] C.M. MacNeill, R.C. Coffin, D.L. Carroll, N.H. Levi-Polyachenko, Low band gap donor-acceptor conjugated polymer nanoparticles and their NIR-mediated thermal ablation of cancer cells, Macromol. Biosci. 13 (2013) 28–34, https://doi.org/10.1002/mabi.201200241.
[142] S. Manohar, A. Kharine, J.C.G. van Hespen, W. Steenbergen, T.G. van Leeuwen, Photoacoustic mammography laboratory prototype: imaging of breast tissue phantoms, J. Biomed. Opt. 9 (2004) 1172–1181, https://doi.org/10.1117/1.1803548.
[143] S.H. Alavi, W.F. Liu, A. Kheradvar, Inflammatory response assessment of a hybrid tissue-engineered heart valve leaflet, Ann. Biomed. Eng. 41 (2013) 316–326, https://doi.org/10.1007/s10439-012-0664-7.
[144] A. Aguirre, Y. Ardeshirpour, M.M. Sanders, M. Brewer, Q. Zhu, Potential role of coregistered photoacoustic and ultrasound imaging in ovarian cancer detection and characterization, Transl. Oncol. 4 (2011) 29–37, https://doi.org/10.1593/tlo.10187.
[145] C. Xie, P.K. Upputuri, X. Zhen, M. Pramanik, K. Pu, Self-quenched semiconducting polymer nanoparticles for amplified in vivo photoacoustic imaging, Biomaterials 119 (2017) 1–8, https://doi.org/10.1016/j.biomaterials.2016.12.004.
[146] Y. Jiang, P.K. Upputuri, C. Xie, Z. Zeng, A. Sharma, X. Zhen, J. Li, J. Huang, M. Pramanik, K. Pu, Metabolizable semiconducting polymer nanoparticles for second near-infrared photoacoustic imaging, Adv. Mater. 31 (2019) 1808166, https://doi.org/10.1002/adma.201808166.
[147] Y. Jiang, P.K. Upputuri, C. Xie, Y. Lyu, L. Zhang, Q. Xiong, M. Pramanik, K. Pu, Broadband absorbing semiconducting polymer nanoparticles for photoacoustic imaging in second near-infrared window, Nano Lett. 17 (2017) 4964–4969, https://doi.org/10.1021/acs.nanolett.7b02106.
[148] L. Wu, X. Cai, K. Nelson, W. Xing, J. Xia, R. Zhang, A.J. Stacy, M. Luderer, G.M. Lanza, L. V Wang, B. Shen, D. Pan, A green synthesis of carbon nanoparticle from honey for real-time photoacoustic imaging, Nano Res. 6 (2013) 312–325, https://doi.org/10.1007/s12274-013-0308-8.
[149] C. Gellini, A. Feis, Optothermal properties of plasmonic inorganic nanoparticles for photoacoustic applications, Photoacoustics 23 (2021) 100281, https://doi.org/10.1016/j.pacs.2021.100281.
[150] C. Sun, L. Wen, J. Zeng, Y. Wang, Q. Sun, L. Deng, C. Zhao, Z. Li, One-pot solventless preparation of PEGylated black phosphorus nanoparticles for photoacoustic imaging and photothermal therapy of cancer, Biomaterials 91 (2016) 81–89, https://doi.org/10.1016/j.biomaterials.2016.03.022.
[151] C. Wu, R. Zhang, W. Du, L. Cheng, G. Liang, Alkaline phosphatase-triggered self-assembly of near-infrared nanoparticles for the enhanced photoacoustic imaging of tumors, Nano Lett. 18 (2018) 7749–7754, https://doi.org/10.1021/acs.nanolett.8b03482.
[152] P.A. Schulte, F. Salamanca-Buentello, Ethical and scientific issues of nanotechnology in the workplace, Environ. Health Perspect. 115 (2007) 5–12, https://doi.org/10.1289/ehp.9456.
[153] N.A. Al-Tayyar, A.M. Youssef, R. Al-hindi, Antimicrobial food packaging based on sustainable Bio-based materials for reducing foodborne Pathogens: a review, Food Chem. 310 (2020) 125915, https://doi.org/10.1016/j.foodchem.2019.125915.
[154] J.F. Jacobs, I. van de Poel, P. Osseweijer, Sunscreens with titanium dioxide (TiO(2)) nano-particles: a societal experiment, Nanoethics 4 (2010) 103–113, https://doi.org/10.1007/s11569-010-0090-y.
[155] S.K. Sardana, V.K. Komarala, Optical properties of hybrid plasmonic structure on silicon using transparent conducting-silver nanoparticles–silicon dioxide layers: the role of conducting oxide layer thickness in antireflection, J. Opt. 18 (2016) 75004, https://doi.org/10.1088/2040-8978/18/7/075004.
[156] N. Shakti, G. P.S, Structural and optical properties of sol-gel prepared ZnO thin film, Appl. Phys. Res. 2 (2010), https://doi.org/10.5539/apr.v2n1p19.
[157] W.H. De Jong, P.J.A. Borm, Drug delivery and nanoparticles:applications and hazards, Int. J. Nanomed. 3 (2008) 133–149, https://doi.org/10.2147/ijn.s596.
[158] F.D. Ledley, Nonviral gene therapy: the promise of genes as pharmaceutical products, Hum. Gene Ther. 6 (1995) 1129–1144, https://doi.org/10.1089/hum.1995.6.9-1129.
[159] C. Yao, Z. Li, Z. Zhang, Study on the fundamental of the laser high-precision microsurgery, Guangxue Xuebao/Acta Opt. Sin. 25 (2005) 1664–1669.
[160] C. Xu, Y. Ying, J. Ping, Colorimetric aggregation assay for kanamycin using gold nanoparticles modified with hairpin DNA probes and hybridization chain reaction-assisted amplification, Mikrochim. Acta 186 (2019) 448, https://doi.org/10.1007/s00604-019-3574-7.
[161] Y. Liu, D. Zhang, E.C. Alocilja, S. Chakrabartty, Biomolecules detection using a silver-enhanced gold nanoparticle-based biochip, Nanoscale Res. Lett. 5 (2010) 533, https://doi.org/10.1007/s11671-010-9542-0.
[162] N. Nazar, I. Bibi, S. Kamal, M. Iqbal, S. Nouren, K. Jilani, M. Umair, S. Ata, Cu nanoparticles synthesis using biological molecule of P. granatum seeds extract as reducing and capping agent: growth mechanism and photo-catalytic activity, Int. J. Biol. Macromol. 106 (2018) 1203–1210, https://doi.org/10.1016/j.ijbiomac.2017.08.126.
[163] I. Yildiz, Applications of magnetic nanoparticles in biomedical separation and purification 5 (2016) 331–340, https://doi.org/10.1515/ntrev-2015-0012.

[164] J. Fan, H. Li, J. Jiang, L.K.Y. So, Y.W. Lam, P.K. Chu, 3C–SiC nanocrystals as fluorescent biological labels, Small 4 (2008) 1058–1062, https://doi.org/10.1002/smll.200800080.
[165] M.M. Mahan, A.L. Doiron, Gold nanoparticles as X-ray, CT, and multimodal imaging contrast agents: formulation, targeting, and methodology, J. Nanomater. 2018 (2018) 5837276, https://doi.org/10.1155/2018/5837276.
[166] S.K. Nitta, K. Numata, Biopolymer-based nanoparticles for drug/gene delivery and tissue engineering, Int. J. Mol. Sci. 14 (2013) 1629–1654, https://doi.org/10.3390/ijms14011629.
[167] W. Zhang, B. Karn, Nanoscale environmental science and technology: challenges and opportunities, Environ. Sci. Technol. 39 (2005) 94A–95A.
[168] A. Hoshino, S. Hanada, K. Yamamoto, Toxicity of nanocrystal quantum dots: the relevance of surface modifications, Arch. Toxicol. 85 (2011) 707–720, https://doi.org/10.1007/s00204-011-0695-0.
[169] S. Lanone, J. Boczkowski, Biomedical applications and potential health risks of nanomaterials: molecular mechanisms, Curr. Mol. Med. 6 (2006) 651–663, https://doi.org/10.2174/156652406778195026.
[170] F. Proffitt, Yellow light for nanotech, Science 305 (2004) 762, https://doi.org/10.1126/science.305.5685.762b.
[171] D. Cui, F. Tian, C.S. Ozkan, M. Wang, H. Gao, Effect of single wall carbon nanotubes on human HEK293 cells, Toxicol. Lett. 155 (2005) 73–85, https://doi.org/10.1016/j.toxlet.2004.08.015.
[172] C.-W. Lam, J.T. James, R. McCluskey, R.L. Hunter, Pulmonary toxicity of single-wall carbon nanotubes in mice 7 and 90 days after intratracheal instillation, Toxicol. Sci. 77 (2004) 126–134, https://doi.org/10.1093/toxsci/kfg243.
[173] B. Banik, B. Surnar, B.W. Askins, M. Banerjee, S. Dhar, Dual-targeted synthetic nanoparticles for cardiovascular diseases, ACS Appl. Mater. Interfaces 12 (2020) 6852–6862, https://doi.org/10.1021/acsami.9b19036.
[174] J.M. Rosenholm, A. Meinander, E. Peuhu, R. Niemi, J.E. Eriksson, C. Sahlgren, M. Lindén, Targeting of porous hybrid silica nanoparticles to cancer cells, ACS Nano 3 (2009) 197–206, https://doi.org/10.1021/nn800781r.
[175] R. Kannan, A. Zambre, N. Chanda, R. Kulkarni, R. Shukla, K. Katti, A. Upendran, C. Cutler, E. Boote, K. V Katti, Functionalized radioactive gold nanoparticles in tumor therapy, Wiley Interdiscip. Rev. Nanomed. Nanobiotechnol. 4 (2012) 42–51, https://doi.org/10.1002/wnan.161.
[176] A.S. Nikolov, N.E. Stankova, D.B. Karashanova, N.N. Nedyalkov, E.L. Pavlov, K.T. Koev, H. Najdenski, V. Kussovski, L.A. Avramov, C. Ristoscu, M. Badiceanu, I. N. Mihailescu, Synergistic effect in a two-phase laser procedure for production of silver nanoparticles colloids applicable in ophthalmology, Opt Laser. Technol. 138 (2021) 106850, https://doi.org/10.1016/j.optlastec.2020.106850.
[177] J.L. Winer, P.E. Kim, M. Law, C.Y. Liu, M.L.J. Apuzzo, Visualizing the future: enhancing neuroimaging with nanotechnology, World Neurosurg 75 (2011) 626–629, https://doi.org/10.1016/j.wneu.2011.02.016.
[178] O. Veiseh, B.C. Tang, K.A. Whitehead, D.G. Anderson, R. Langer, Managing diabetes with nanomedicine: challenges and opportunities, Nat. Rev. Drug Discov. 14 (2015) 45–57, https://doi.org/10.1038/nrd4477.
[179] A. Rocca, S. Moscato, F. Ronca, S. Nitti, V. Mattoli, M. Giorgi, G. Ciofani, Pilot in vivo investigation of cerium oxide nanoparticles as a novel anti-obesity pharmaceutical formulation, Nanomedicine 11 (2015) 1725–1734, https://doi.org/10.1016/j.nano.2015.05.001.
[180] J.K. Vasir, V. Labhasetwar, Quantification of the force of nanoparticle-cell membrane interactions and its influence on intracellular trafficking of nanoparticles, Biomaterials 29 (2008) 4244–4252, https://doi.org/10.1016/j.biomaterials.2008.07.020.
[181] D.M. Smith, J.K. Simon, J.R. Baker Jr., Applications of nanotechnology for immunology, Nat. Rev. Immunol. 13 (2013) 592–605, https://doi.org/10.1038/nri3488.
[182] P.K. Upputuri, M. Pramanik, Fast photoacoustic imaging systems using pulsed laser diodes: a review, Biomed. Eng. Lett. 8 (2018) 167–181, https://doi.org/10.1007/s13534-018-0060-9.
[183] T.J. Allen, P.C. Beard, High power visible light emitting diodes as pulsed excitation sources for biomedical photoacoustics, Biomed. Opt Express 7 (2016) 1260–1270, https://doi.org/10.1364/BOE.7.001260.
[184] K. Daoudi, P.J. van den Berg, O. Rabot, A. Kohl, S. Tisserand, P. Brands, W. Steenbergen, Handheld probe integrating laser diode and ultrasound transducer array for ultrasound/photoacoustic dual modality imaging, Opt Express 22 (2014) 26365–26374, https://doi.org/10.1364/OE.22.026365.
[185] M. Kuniyil Ajith Singh, W. Steenbergen, Photoacoustic-guided focused ultrasound (PAFUSion) for identifying reflection artifacts in photoacoustic imaging, Photoacoustics 3 (2015) 123–131, https://doi.org/10.1016/j.pacs.2015.09.001.
[186] R.G.M. Kolkman, P.J. Brands, W. Steenbergen, T.G.C. van Leeuwen, Real-time in vivo photoacoustic and ultrasound imaging, J. Biomed. Opt. 13 (2008) 50510, https://doi.org/10.1117/1.3005421.
[187] Y. Xin, H. Sun, H. Tian, C. Guo, X. Li, S. Wang, C. Wang, The use of polyvinylidene fluoride (PVDF) films as sensors for vibration measurement: a brief review, Ferroelectrics 502 (2016) 28–42, https://doi.org/10.1080/00150193.2016.1232582.
[188] A. Garcia-Uribe, T.N. Erpelding, A. Krumholz, H. Ke, K. Maslov, C. Appleton, J.A. Margenthaler, L. V Wang, Dual-modality photoacoustic and ultrasound imaging system for noninvasive sentinel lymph node detection in patients with breast cancer, Sci. Rep. 5 (2015) 15748, https://doi.org/10.1038/srep15748.
[189] R. Manwar, K. Kratkiewicz, K. Avanaki, Overview of ultrasound detection technologies for photoacoustic imaging, Micromachines 11 (2020), https://doi.org/10.3390/mi11070692.
[190] H. Ke, T.N. Erpelding, L. Jankovic, C. Liu, L. V Wang, Performance characterization of an integrated ultrasound, photoacoustic, and thermoacoustic imaging system, J. Biomed. Opt. 17 (2012) 56010, https://doi.org/10.1117/1.JBO.17.5.056010.
[191] S. Noimark, R.J. Colchester, B.J. Blackburn, E.Z. Zhang, E.J. Alles, S. Ourselin, P.C. Beard, I. Papakonstantinou, I.P. Parkin, A.E. Desjardins, Carbon-nanotube–PDMS composite coatings on optical fibers for all-optical ultrasound imaging, Adv. Funct. Mater. 26 (2016) 8390–8396, https://doi.org/10.1002/adfm.201601337.
[192] S. Manohar, C. Ungureanu, T.G. Van Leeuwen, Gold nanorods as molecular contrast agents in photoacoustic imaging: the promises and the caveats, Contrast Media Mol. Imaging 6 (2011) 389–400.
[193] X. Liang, W. Shang, C. Chi, C. Zeng, K. Wang, C. Fang, Q. Chen, H. Liu, Y. Fan, J. Tian, Dye-conjugated single-walled carbon nanotubes induce photothermal therapy under the guidance of near-infrared imaging, Cancer Lett. 383 (2016) 243–249.
[194] Z. Zha, Z. Deng, Y. Li, C. Li, J. Wang, S. Wang, E. Qu, Z. Dai, Biocompatible polypyrrole nanoparticles as a novel organic photoacoustic contrast agent for deep tissue imaging, Nanoscale 5 (2013) 4462–4467.
[195] H.F. Zhang, K. Maslov, G. Stoica, L.V. Wang, Functional photoacoustic microscopy for high-resolution and noninvasive in vivo imaging, Nat. Biotechnol. 24 (2006) 848–851.
[196] H.-W. Yang, H.-L. Liu, M.-L. Li, I.-W. Hsi, C.-T. Fan, C.-Y. Huang, Y.-J. Lu, M.-Y. Hua, H.-Y. Chou, J.-W. Liaw, Others, Magnetic gold-nanorod/PNIPAAmMA nanoparticles for dual magnetic resonance and photoacoustic imaging and targeted photothermal therapy, Biomaterials 34 (2013) 5651–5660.
[197] Y.-S. Chen, D. Yeager, S.Y. Emelianov, Photoacoustic imaging for cancer diagnosis and therapy guidance, in: Cancer Theranostics, Elsevier, 2014, pp. 139–158.
[198] J. Zhong, L. Wen, S. Yang, L. Xiang, Q. Chen, D. Xing, Imaging-guided high-efficient photoacoustic tumor therapy with targeting gold nanorods, Nanomed. Nanotechnol. Biol. Med. 11 (2015) 1499–1509.
[199] A. Zare, P. Shamshiripour, S. Lotfi, M. Shahin, V.F. Rad, A.-R. Moradi, F. Hajiahmadi, D. Ahmadvand, Clinical theranostics applications of photo-acoustic imaging as a future prospect for cancer, J. Contr. Release 351 (2022) 805–833.
[200] L. Xie, G. Wang, H. Zhou, F. Zhang, Z. Guo, C. Liu, X. Zhang, L. Zhu, Functional long circulating single walled carbon nanotubes for fluorescent/photoacoustic imaging-guided enhanced phototherapy, Biomaterials 103 (2016) 219–228.
[201] R. Cheheltani, R.M. Ezzibdeh, P. Chhour, K. Pulaparthi, J. Kim, M. Jurcova, J.C. Hsu, C. Blundell, H.I. Litt, V.A. Ferrari, Others, Tunable, biodegradable gold nanoparticles as contrast agents for computed tomography and photoacoustic imaging, Biomaterials 102 (2016) 87–97.
[202] S.W. Yoo, D. Jung, J.-J. Min, H. Kim, C. Lee, Biodegradable contrast agents for photoacoustic imaging, Appl. Sci. 8 (2018) 1567.
[203] Q. Miao, K. Pu, Emerging designs of activatable photoacoustic probes for molecular imaging, Bioconjugate Chem. 27 (2016) 2808–2823.
[204] H. Deng, H. Qiao, Q. Dai, C. Ma, Deep learning in photoacoustic imaging: a review, J. Biomed. Opt. 26 (2021), 040901–040901.
[205] P.J. Van den Berg, K. Daoudi, W. Steenbergen, Review of photoacoustic flow imaging: its current state and its promises, Photoacoustics 3 (2015) 89–99.